

Student thesis series INES nr 289

Centennial and Millennial climate-carbon cycle feedback analysis for future anthropogenic climate change

Dipa Paul Chowdhury

2013

Department of
Physical Geography and Ecosystems Science
Lund University
Sölvegatan 12
S-223 62 Lund
Sweden



Dipa Paul Chowdhury (2013). Centennial and Millennial climate-carbon cycle feedback analysis for future anthropogenic climate change
Master degree thesis, 30 credits in *Physical Geography and Ecosystem Analysis*
Department of Physical Geography and Ecosystem Science, Lund University

Centennial and Millennial climate-carbon cycle feedback analysis for future anthropogenic climate change

Dipa Paul Chowdhury
Master degree 30 credits thesis in
Physical Geography and Ecosystem Analysis

Supervisor: Guy Schurgers
Department of Physical Geography & Ecosystems Analysis
Lund University

Abstract

Increased anthropogenic emission of CO₂ is alleged to impact the climate system in the future, which will affect the feedback between carbon cycle and climate change. In this project, a climate-carbon cycle feedback analysis has been conducted by using long simulated time series (2001 – 3000) data, derived from the Max-Planck-Institute / University of Wisconsin-Madison Earth System Model (MPI/UW ESM). This complex Earth system model was forced by historical emissions of CO₂ and by three IPCC SRES scenarios, A2, A1B and B1 till 2100, then for the remainder (2100-3000), an exponential decrease of CO₂ emissions was assumed. The analysis has been calculated for the 21st century and for the year 3000, to study the short term (100 year) and long term (1000 year) climate-carbon cycle feedback. In addition, there is not only a difference in time period but also centennial time scale represents a transient state where CO₂ forcing continues to increase; on the other hand millennium time scale represents a near equilibrium state of the Earth system against CO₂ forcing. For both the centennial and millennial time scale, this complex Earth system model results in positive feedbacks between carbon cycle and climate change for all three scenarios (A2, A1B, and B1). The magnitude of this positive feedback will be stronger by the end of the millennium (3000). This positive feedback clearly indicates that climate change will reduce the carbon uptake by the Earth system due to the climate carbon cycle feedback, thus there will be more remaining CO₂ in the atmosphere which is able to produce an additional warming on climate system. The relative magnitude of this positive feedback varies depending on scenarios. For the A2 scenario, this positive feedback has increased by 9% and 39% for 21st century, and for the year 3000, respectively compared to the 20th century. For the A1B scenarios, it has increased by 10% and 30%, respectively, and for the B1 scenario, it has increased by 7% and 14% correspondingly.

Keywords: Earth system model, climate change, carbon cycle, feedback, scenario, sensitivity.

Contents

Abstract	iv
1. Introduction	1
1.1. Aim and objectives	4
2. Background	5
2.1. Carbon Cycle.....	5
2.2. Anthropogenic CO ₂ and Climate change effect on carbon cycle.....	9
2.3. Feedback.....	12
2.4. Climate-carbon cycle feedback system.....	14
3. Methodology	19
3.1. Model description.....	19
3.2. Data description.....	21
3.3. Analysis.....	24
3.4. Method to analyze feedback.....	25
4. Results	32
4.1. Global carbon budget observed on recent past decades.....	32
4.2. Global carbon budget for the future.....	35
4.2.1. Estimation of carbon budget for the year of 2100 and 3000	35
4.2.2. Changes in growth rate over time: decade by decade from 2001 to 3000.....	36
4.2.3. Simulated fraction of carbon emissions into air, land and ocean.....	39
4.3. Climate change effect on carbon cycle.....	40
4.3.1. Climate change effect: Land uptake versus ocean uptake.....	42
4.4. Climate-carbon cycle feedback analysis: short term versus long term.....	44
4.4.1. Quantifying main component sensitivities of the climate carbon cycle feedback.....	45
4.4.2. Feedback factor and gain of the climate carbon cycle feedback.....	48
4.4.3. Comparison with other studies.....	50
4.4.4. Changes in sensitivity components over time: decade by decade from 2001 to 3000.....	51
4.4.5. Changes in feedback factor and gain over time: decade by decade from 2001 to 3000.....	55
4.5. Strength of climate change and carbon cycle separately on climate-carbon cycle feedback.....	57
5. Discussion	60
5.1. Limitation of the study.....	60
5.2. Model sensitivity to quantify feedback.....	61
5.3. Difference in land and ocean carbon cycle response.....	64
6. Conclusion	66
Acknowledgements	69
References	69

1. Introduction

The physical climate system and the global carbon cycle, both the terrestrial and the marine component, are interlinked, so that changing one of them affects others. The Earth's climate is a dynamic complex system and is regulated by continuous inter-connected physical, chemical and biological processes occurring in atmosphere, biosphere, ocean and cryosphere. The changes in the climate system are determined through different external factors which can be either natural or man-made and these factors are known as 'forcings'. Some of the natural forcings are solar irradiance changes, volcanic eruptions and man-made forcings include the emissions of different type of trace gases into the atmosphere (Le Treut et al., 2007).

The most important trace gases with potential to alter the radiative properties of the climate system are long lived greenhouse gases (GHGs) such as Carbon-di-oxide (CO₂), methane (CH₄) and nitrous oxide (N₂O) (Forster et al., 2007). The awareness about the greenhouse gases in the atmosphere has been established more than 150 years and since then, CO₂ is identified as greenhouse gas (Tyndall, 1861; Arrhenius, 1896). The CO₂ concentration was approximately 260 ppm 10 thousand years ago which had increased by only 20 ppm up to the pre-industrial time. However, a continuous increase of CO₂ has been observed since the beginning of the industrial era, 1750 (Jansen et al., 2007; Denman et al., 2007). Direct instrumental measurement of CO₂ concentration has started from 1958 on Mauna Loa Observatory in Hawaii under the supervision of Charles David Keeling (Keeling, 1960). In the first measurement (1959) and at present (2012), the mean annual CO₂ concentration was 315 and 393 ppm respectively (Scripps Institution of Oceanography, 2013): CO₂ concentration has increased more than 100 ppm in the last 250 years in comparison to its pre-industrial (10 thousand years) period. The growth rate of CO₂ in any year indicates the average increase of CO₂ for that year than the previous year. The annual atmospheric CO₂ growth rate of last decade 2003-2012 was 2.07 ppm yr⁻¹ which was the highest ever recorded growth rate of last five decades (Table 1).

Table1: Growth rate of CO₂ per decade (1963-2012)

Decades	Growth rate of CO ₂ (ppm yr ⁻¹)
1963-1972	0.90
1973-1982	1.37
1983-1992	1.52
1993-2002	1.67
2003-2012	2.07

Source: Scripps Institution of Oceanography, 2013

The reason for this drastically increasing trend of CO₂ concentration in the atmosphere are human activities, and it has been shown by analyzing the nature of carbon isotope available in the atmosphere that the origin of present atmospheric CO₂ is from fossil fuel (Keeling, 1960). Major anthropogenic sources are fossil fuel combustion (uses in transportation, heating and cooling system of the houses) and cement productions, which together contribute more than 75% of present anthropogenic CO₂ concentration since pre-industrial period (Denman et al., 2007). Different land use changes (e.g. deforestation, agricultural practices) are contributing the rest.

In reality, the current status of atmospheric CO₂ concentrations does not disclose the full degree of anthropogenic emissions, as land and ocean continuously taken up carbon from the atmosphere. Enhanced atmospheric CO₂ concentration can result in higher primary production of terrestrial plants under the condition of available water and nutrient which is termed as 'CO₂ fertilization effect' (Gifford, 1994). Also, oceanic carbon uptake may increase by increased dissolution of CO₂ with higher concentration of atmospheric CO₂ (Feely et al., 2004). Thus, this increased atmospheric CO₂ concentration may increase the carbon stock of terrestrial ecosystem and ocean through different biophysical and biochemical processes. Since 1959 to present time, almost half of the atmospheric CO₂ emissions have been consumed by land and ocean ecosystem and the other half (approximately 55%) has remained in the atmosphere (Denman et al., 2007). However this uptake of carbon by land and ocean is not only dependent on CO₂ fertilization but also affected by CO₂-induced climate change as well.

The direct effects of CO₂ on temperature are relatively well studied and understood. The extra amount of CO₂ in the atmosphere has direct impact on the Earth's radiation balance through the greenhouse effect (Hansen et al., 1981). Many studies show that climate change through increased temperature can significantly reduce the efficiency of carbon uptake of terrestrial ecosystem (Cox et al., 2000; Cramer et al., 2001; Schurgers et al., 2008) and ocean (Bopp et al., 2001; Archer et al., 2004; Joos et al., 2001) by accelerating many biogeochemical processes (e.g. respiration) which can contribute to an increase of the airborne fraction of CO₂ (Cao and Woodland 1998, Davidson and Janssens 2006). Therefore, climate change affects CO₂ fluxes through photosynthesis, respiration, dissolution of CO₂ and in return, atmospheric CO₂ concentration itself is affected (Cox et al., 2000 and Joos et al., 2001).

Now, under increased anthropogenic emission of CO₂, land and ocean can probably sink more CO₂ through changes in soil, photosynthesis process in vegetation and dissolution in the surface ocean. However, both land and ocean systems may gradually saturate as this sinking process cannot be continued forever. On the other hand, the effect of temperature (or climate change) is much less understood. Marine and land carbon uptake processes may be affected by the increased temperature or climate change (Dufresne et al., 2002).

Several climate model studies have shown that this anthropogenic CO₂ emission may have substantial effect on the climate system for coming centuries (Platter et al., 2008; Houghton et al., 2001). Terrestrial ecosystems and oceans do not respond in the same way under the predicted high load of CO₂ concentration and consequent future climate change. For shorter time scale (e.g. decade, century), the terrestrial carbon cycle may be more dominant than the marine carbon cycle in taking up carbon, as many of the oceanic process such as deposition of CaCO₃ on deep ocean takes few century to thousand years and weathering takes more than thousands years (Archer et al., 2008; Eby et al., 2009). Thus, the state of climate-carbon cycle feedback is affected differently at different timescales. So, the changes in the global carbon cycle will be determined by the future emission, consequent climate change and the response of land and ocean carbon cycle to climate change and CO₂ concentration.

Different climate model simulations with different levels of complexity have been conducted to study and describe the long-term effects of increased anthropogenic CO₂ on the land and ocean carbon cycle and future climate change. Most of the climate models have been applied to simulate climate change till the 21st century by integrating different IPCC emission scenarios for future anthropogenic CO₂ emission (Cox et al., 2000; Dufresne et al., 2002; Friedlingstein et al., 2003). A complex Earth system model consisting atmosphere, ocean and land carbon cycle and ice-sheets has been established to study century to millennium timescale response of climate change to future anthropogenic CO₂ emissions and consequent effect on carbon stock of terrestrial and marine environment (Winguth et al., 2005, Mikolajewicz et al., 2006, Schurgers et al., 2008). This model was used to simulate three different scenarios (A1B, A2, and B1) from the Special Report on Emission Scenarios (SRES) (Nakićenović et al., 2001) by the Intergovernmental panel on climate change (IPCC) which was available till the 21st century. After the 21st century, these simulations have been continued under the assumption that anthropogenic

CO₂ emission will start to reduce and as a result, the coupling of climate-carbon cycle will shift to a new equilibrium state by the end of this millennium (Mikolajewicz et al., 2006).

The goal of this project is to quantify the climate-carbon cycle feedback through time by using long simulated time series (2001 – 3000) data, derived from this complex Earth system model (ESM). The feedback analysis of climate-carbon cycle up to the 21st century has been conducted in previously published studies (Friedlingstein et al., 2003; Friedlingstein et al., 2006). However, this project will conduct the climate-carbon cycle feedback analysis beyond the 21st century till the end of this millennium. Therefore, it will be possible to observe how the climate-carbon cycle feedback changes from centennial to millennium time scale.

1.1. Aim and objectives

The following research question is addressed in this project:

- ‘How does the climate-carbon cycle feedback affect climate change and carbon cycle on centennial and millennial timescales under the influence of CO₂-induced future anthropogenic climate change?’

To answer this question, the following objectives of the project were set:

1. To estimate and compare the future global carbon budget for shorter (100) and longer (1000) timescales under different emission scenarios.
2. To analyze how the terrestrial and marine carbon storage are influenced by future anthropogenic climate change.
3. To quantify the sensitivity of climate-carbon cycle feedback in the Max-Planck-Institute / University of Wisconsin-Madison Earth System Model (MPI/UW ESM), and compare this with other studies.
4. To investigate whether CO₂ concentration or climate changes act as dominating factors in the climate-carbon cycle feedback system.

It is possible to explore how all the above stated objectives evolved for three different emission scenarios (A1B, A2, and B1) from the SRES report (Nakićenović et al., 2001), which were used in the model (MPI/UW Earth System Model) as prescribed future anthropogenic CO₂ emissions.

2. Background

2.1. Carbon Cycle

Carbon, being the fourth most abundant elements in the Earth system, is the basic chemical element for all the organic compounds. Carbon-based compounds are the basis for forming most of the biological compounds (e.g. DNA) which sustains the existence of life (NASA, 2011). Thus, the carbon cycle is considered as one of the most important biogeochemical cycles in the Earth system. The carbon can stay in different forms (e.g. CO_2 , CO_3^{2-}) in the Earth system depending on reservoirs. The major reservoirs of carbon in the Earth are atmosphere, oceans, lithosphere, terrestrial biosphere, aquatic biosphere and fossil (Falkowski et al., 2000; Fig. 1). Carbon circulates through all these carbon pools (Fig. 2). Among all the reservoirs, the lithosphere is the largest reservoirs (Fig. 1) where 80% of the Earth's carbon is stored as limestone and its derivatives through sedimentation of calcium carbonate from the shell of dead marine organisms and the rest of it as kerogens, which are formed from the sedimentation of dead terrestrial organisms (NASA, 2011). The carbon moves very slowly between the atmosphere and lithosphere through chemical weathering and tectonic activity which takes 100-200 million years, which is known as the slow carbon cycle (Falkowski et al., 2000; NASA, 2011). Carbon releases naturally from the lithosphere to the atmosphere through volcanic eruptions with subduction of tectonic plates (Berner, 2003). In contrast to this natural phenomenon, more carbon is released from the fossil fuels due to the increased combustion of coal, oil and gas by human (Denman et al., 2007).

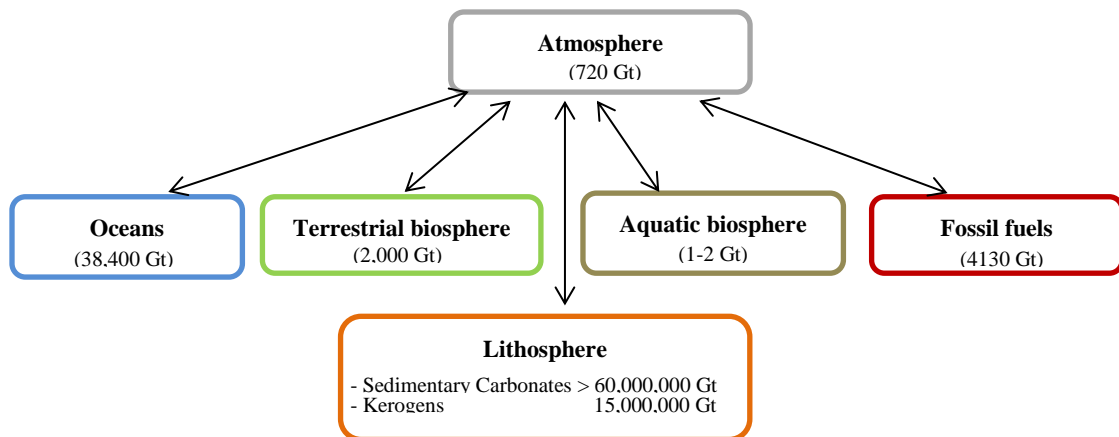


Figure 1: Distribution (approximate) of global carbon pools (Gt) in major reservoirs on the Earth (modified from Falkowski et al., 2000).

The ocean is the second largest reservoir after the lithosphere (Fig. 1), which is considered as the largest active pool of carbon. The ocean and terrestrial biosphere are regarded as the active carbon reservoirs for their rapid exchange of CO₂ with the atmosphere (Lal, 2004; Falkowski et al., 2000).

The carbon exchanges among reservoirs through various physical, chemical, biological and geological processes which take place on different time periods, ranging from hours to millions of years. The century to millennium timescale processes include photosynthesis, respiration, dissolution of CO₂ into seawater and humus accumulation. However, the processes which takes over millions of years include weathering, storage of dissolved inorganic carbon (DIC) in deep ocean, sedimentation of dead terrestrial organism to form kerogens, formation of fossil fuels (Berner, 2003).

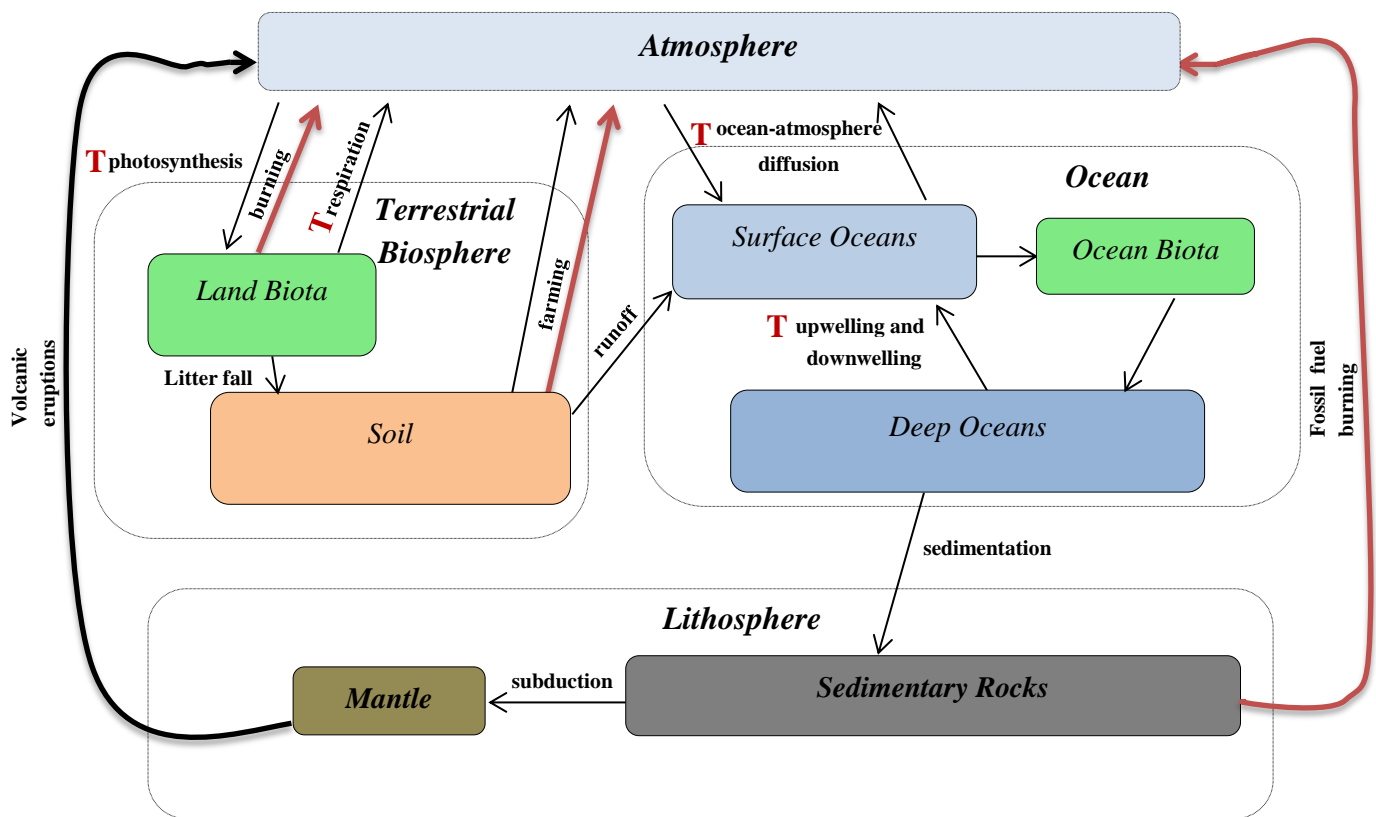


Figure 2: The Global Carbon Cycle (modified from Bice, 2012), flows with red arrows are indicating human influence on carbon emission and red T indicates flows sensitive to temperature.

Changes in the global carbon cycle at a century to millennium timescale are mainly originating from the emission of atmospheric CO₂ and the response of terrestrial and ocean carbon cycle to the amount of available atmospheric CO₂. In return, the rate of atmospheric CO₂ change is determined by the uptake of carbon by terrestrial biosphere and ocean (Prentice et al., 2001).

Terrestrial Carbon Cycle: In the terrestrial carbon cycle, carbon exchanges through different terrestrial reservoirs, especially through living terrestrial biomass and soil (Fig. 2). The total carbon stored in terrestrial ecosystems as living and dead biomass is approximately three times larger than the atmospheric carbon pool (Fig. 1). The carbon uptake from the atmosphere in the terrestrial ecosystem is regulated by photosynthesis and released in the atmosphere by autotrophic (by plant) respiration and heterotrophic (microbial decomposition of dead organic matter) respiration.

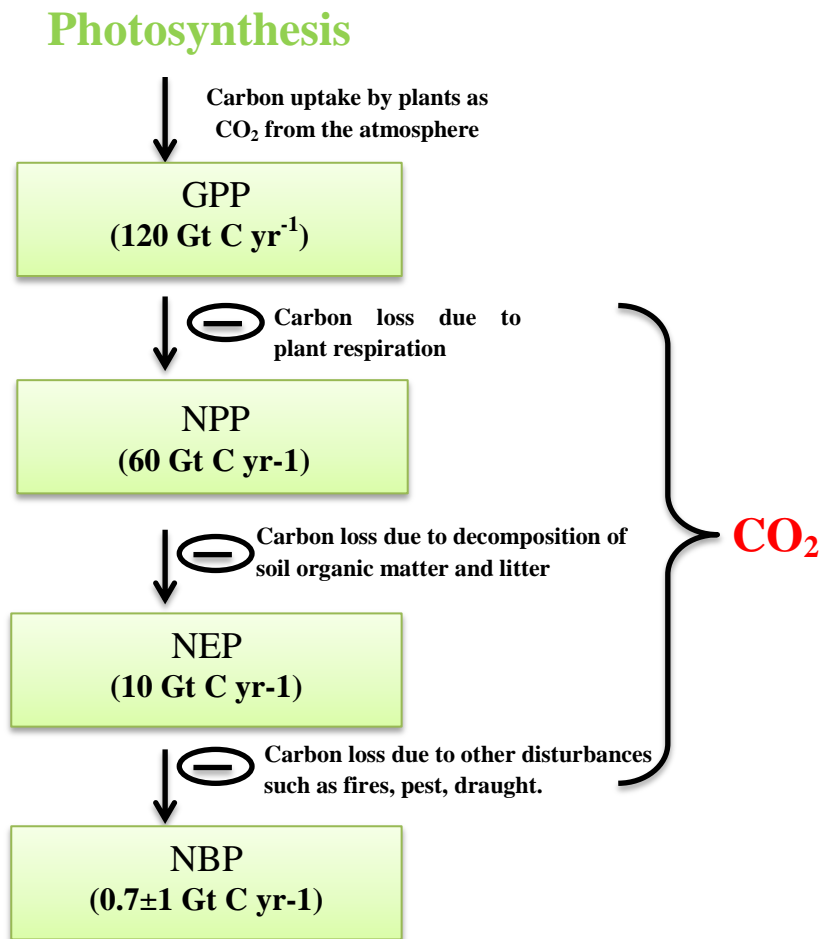


Figure 3: Simplified terrestrial global carbon balance, modified from IPCC (2000).

The total carbon uptake by plants through photosynthesis is the gross primary production (GPP). Net primary production (NPP) of any terrestrial ecosystem is estimated by the net uptake (the difference between GPP and autotrophic respiration) of atmospheric CO₂ as the organic carbon; net ecosystem production (NEP) is the difference between NPP and heterotrophic respiration. In addition, there is carbon loss into the atmosphere due to disturbances such as fires, drought, and human activities. Now, NEP after excluding the carbon loss from the disturbances is known as net biome production (NBP). Therefore, NBP represents the net carbon exchange between atmosphere and the terrestrial biosphere (Fig. 3) (Cao and Woodward, 1998).

Ocean Carbon Cycle: The ocean carbon cycle is the exchange of carbon among the atmosphere and oceans (Fig. 2). Oceans contain 50 times more carbon than the atmosphere (Fig. 1). In the ocean water, carbon can exist in various forms such as dissolved inorganic carbon (DIC), dissolved organic carbon (DOC) and particulate organic carbon (POC) and the approximate ratio of their existence is DIC:DOC:POC = 2000:38:1 (Denman et al., 2007).

Heinze et al., (1991) have identified three key ocean carbon pumps which can explain how the atmospheric CO₂ can exchange with the ocean. These are: (a) solubility pump, (b) organic carbon pump and (c) CaCO₃ ‘counter pump’. As CO₂ is a weak acidic gas and ocean water is slightly alkaline, ocean surface water can absorb huge amounts of atmospheric CO₂ for its buffering capability in order to neutralize the acidity of CO₂.

Chemically, CO₂ reacts with ocean water to produce carbonic acid (H₂CO₃) (Eq. a) which can split up into a hydrogen ion (H⁺) and bicarbonate (HCO₃⁻) (Eq. b). Afterwards, this hydrogen ion reacts with the carbonate (CO₃²⁻) ion to form one more bicarbonate (Eq. c).



Bicarbonate (inorganic carbon)-rich ocean water is mostly found in high latitudes during the cold season because of its high solubility in cold ocean water which can sink from surface layer to deep ocean through the Meridional Overturning circulation (MOC), and this is referred as

‘solubility pump’ (Denman et al., 2007). However, atmospheric CO₂ can also be taken up by the phytoplankton for photosynthesis which either sinks as dead plant or transformed into DOC (known as organic carbon pump). In this process, some carbon in the sinking particles (dead plant) are respired by bacteria in the surface or intermediate layer of the ocean and recycled as DIC in the surface ocean. The remaining small fraction of particles reaches the deep ocean and during this sinking some is re-suspended, and some is buried at the sea floor. Ocean organisms that have shells (rich of calcium) use bicarbonate (HCO₃⁻) ions to form their calcareous shell (CaCO₃) and in this process CO₂ is released as by product. As this process counters the CO₂ effect, this is called ‘CaCO₃ counter pump’ (Prentice et al., 2001; Denman et al., 2007).

2.2. Anthropogenic CO₂ and associated climate change effect on carbon cycle

In general, the climate of any region refers to the averaged weather condition of that region and climate change refers to the observational changes of climate over a longer time period (decade to millions of years). The carbon cycle has influence on the Earth system for its contribution to the changes in the climate system. The carbon cycle is thus considered an important part of the climate system. The changes in the climate system can be attributed through direct or indirect internal and external forcing which can occur for natural reason or human contribution (Le Treut et al., 2007).

Due to the increased emissions of GHGs (e.g. CO₂, N₂O, CH₄) in the atmosphere, the radiative forcing (RF) at the top the Earth surface (tropopause) has increased considerably since 1750. It has been observed that over the last 250-year period, global atmospheric CO₂ has increased approximately 36% in comparison to its pre-industrial level (Forster et al., 2007). In 2005, measured RF of CO₂ was highest (+1.66 Wm⁻²) among all GHGs (Forster et al., 2007), which implies that the Earth radiation balance has been perturbed from its normal state. As a consequence, the climate system responds by increasing the global mean temperature for adjusting the radiation balance of the Earth’s surface which is termed as greenhouse effect (Denman et al., 2007).

Carbon isotope studies have shown that this increased CO₂ has originated from burning of fossil fuels due to industrialization (Keeling, 1960; Keeling, 1973). Therefore, undoubtedly this

unnatural increasing pattern of CO₂ and associated climate change is due to human activities and can be termed as ‘anthropogenic climate change’. Anthropogenic emission of CO₂ has two main fractions, one is from combustion of fossil fuel and cement production; the other is from deforestation and different agricultural practices (Denman et al., 2007). Before the industrial revolution, most of the changes in the carbon cycle were due to natural causes rather than human contribution. However, now the perturbation of the carbon cycle is mainly due to excess emissions of CO₂ from anthropogenic sources compared to natural changes.

Newly emitted atmospheric CO₂ first distributes in short lived components of the terrestrial biosphere and surface ocean and then re-distributes as long-lived components of terrestrial biosphere and deep ocean (Archer, 2005; Archer and Brovkin, 2008).

Terrestrial Carbon Cycle: The three main physiological processes of terrestrial carbon cycle are plant photosynthesis, autotrophic (due to plant metabolism) and heterotrophic (due to decomposition by soil micro-organism) respiration, which are controlled by various environmental factors such as temperature and precipitation. Three main drivers that can affect the terrestrial carbon cycle are: (a) climate change impact through changes in temperature, precipitation pattern etc., (b) changes in atmospheric composition (e.g. CO₂ fertilization) and (c) land use changes through deforestation or agricultural development (Denman et al., 2007). Thus, the CO₂ concentration increased due to human contribution and the associated climate change may affect terrestrial carbon cycle indirectly.

It has been shown in many studies that enhanced atmospheric CO₂ concentration can result in higher NPP under the prevailing availability of water and nutrients which is termed as ‘CO₂ fertilization effect’ (Gifford, 1994; DeLucia et al., 1999). The CO₂ fertilization effect may decline as NPP is found to saturate with increased CO₂ in future (Cao and Woodward, 1998; King et al., 1997). However, at the same time this enhanced CO₂-induced climate change may affect the respiration processes. Microbial decomposition of dead organic matter is expected to accelerate with increased temperature and reduce the carbon stock (Bond-Lamberty et al., 2004; Knorr et al., 2005). Therefore, the increased terrestrial carbon stock due to the CO₂ fertilization effect is partly offset by this climate change effect, which can potentially reduce the total land carbon stock.

Ocean Carbon Cycle: Most of our Earth surface is covered by ocean which can store more carbon than other reservoirs. Moreover, oceans have great capacity to store more carbon for the presence of carbonate chemistry in seawater which may have the potential to take up extra amount of currently emitted anthropogenic CO₂.

Naturally, atmospheric CO₂ can be rapidly taken up by the surface ocean due to its solubility and buffering capacity, thus the ocean can sink huge amounts of carbon. The quantity of DIC (mostly bicarbonate) in the surface ocean increases with increased anthropogenic CO₂ as the dissolution of CO₂ in seawater also enhances (Sarmiento and Le Quéré, 1996). Moreover, marine ecosystems produce half of the world NPP by using atmospheric CO₂ which ultimately stores as organic carbon in the ocean. The capacity of storing more organic carbon by ocean may enhance due to expected higher photosynthesis by phytoplankton because of increased anthropogenic CO₂ (Field et al., 1998).

However, this increased atmospheric CO₂ may enhance ocean temperature as well and affect carbon exchange with the atmosphere as CO₂ solubility in ocean water is temperature sensitive (Archer et al., 2004). Warmer water outgasses CO₂ and cooler water tends to take up more CO₂ from the atmosphere. The ocean temperature at a depth of 700 m has been reported to have increased by 0.10°C in 42 years (1961-2003) (Bindoff et al., 2007). Thus, this increased warm ocean water may tend to outgas more CO₂ into the atmosphere. Moreover, warm surface ocean water is less dense than the underlying cold saltier water which leads to stratification in ocean water. This stratified ocean water reduces vertical mixing of water which will limit the upward and downward transportation of carbon by impeding nutrient supply in the surface ocean and reduced oxygen supply in the deep ocean (Prentice et al., 2001). Therefore, carbon sequestration by oceans is likely to reduce due to anthropogenic climate change (Sarmiento et al., 1998; Joos et al., 1999).

In the surface ocean, CO₂ stays as three DIC forms: nonionic dissolved CO₂, bicarbonate (HCO₃⁻) and carbonate (CO₃²⁻) and among them 91% are in bicarbonate form (Denman et al., 2007; Goodwin et al., 2009). The amount of this bicarbonate further increases (Eq. a, b, c), but the quantity of carbonates decrease (Eq. c) which will eventually limit the buffering process and most of the additional CO₂ will remain in its dissolved form. In addition, due to reduced buffering process more hydrogen ion remains in the seawater which leads to acidification of

ocean water (Caldeira and Wickett, 2003; Orr et al., 2005). The increased acidification may have two important consequences for ocean ecosystems. First, the biological production of many calcifying organisms will be limited due to less available carbonate ion. Secondly, on longer timescales (e.g. millennial timescales), this acidification can enhance the release of carbonate ions due to dissolution of many shells of marine organism (rich of CaCO_3) or the dissolution from CaCO_3 rich deep ocean sediment. Thus the ocean water will ultimately become more alkaline by advancing the uptake of excess CO_2 from the atmosphere (Lenton and Britton, 2006; Feely et al., 2004). However, these processes vary with century to millennium time scale.

2.3. Feedback

Different feedback mechanisms are playing important roles in the Earth system dynamics, especially in the climate system. It has not been so long that various studies have started to quantify the importance of feedbacks in the climate system and analyze its potential influence on Earth system. The term feedback came to climate study research around 1960s period (Bates, 2007). However, currently it is an important and widespread topic in climate research as future anthropogenic climate change is believed to enhance more due to various feedback mechanisms (Denman et al., 2007).

In general, feedback refers to any change in a component 'X' of a system which can affect other components in a way that the component 'X' in return is affected. The changes in the component X can be either strengthening the initial changes more or further dampening from its the initial stage. Thus, feedbacks can be categorized into two types: (a) positive or amplifying feedbacks and (b) negative or dampening feedbacks. Some important climate feedbacks are water vapor, cloud feedback, and feedbacks between climate and biogeochemical cycles (Bates, 2007).

Quantifying climate feedback:

For observing the consequence of feedbacks and determining their importance in the Earth system, it is necessary to estimate the possible magnitude of feedback for any perturbation in the climate system. The following feedback quantification process is used from the concepts given by Roe (2009):

The Earth's energy budget is determined by the balance between incoming shortwave radiation and outgoing long wave radiation. In equilibrium state, the radiation imbalance at the top of the atmosphere will be zero, meaning all the incoming shortwave radiation will re-radiate as long wave radiation to the space.

For any perturbation in the climate system, the radiative forcing and the global temperature will change. For the additional radiative forcing (in Wm^{-2}) denotes as ΔR_f , the system will reach a new equilibrium state by producing a temperature change ΔT (in K). Therefore,

$$\Delta T = \lambda \Delta R_f \dots\dots\dots (1)$$

Where λ is the climate sensitivity parameter (in K/ Wm^{-2}).

Now, if the system includes any feedback mechanism, there will be an additional temperature change which will be a function of the system response (Roe, 2009). Therefore,

$$\Delta T = \lambda (\Delta R_f + C_1 \Delta T) \dots\dots\dots (2)$$

Where $C_1 \Delta T$ represents additional radiative forcing caused by the feedback, it is assumed to be a linear function of temperature change, ΔT . C_1 is a constant in the equation which determines the feedback strength.

Equation (2) can be re-organized in the following way:

$$\Delta T = \frac{\lambda \Delta R_f}{1 - C_1 \lambda} \dots\dots\dots (3)$$

In this equation, $C_1 \lambda$ is termed as feedback factor, f , and it is a unitless number.

According to Roe (2009), the feedback factor f can be defined as that part of the system output which can be added to the system as input again. ΔT is the temperature change with feedback and ' $\lambda \Delta R_f$ ' is the temperature change without any feedback in the system, renamed here as ΔT_0 for rest of the calculation. Therefore equation (3) can be written as follows:

$$\frac{\Delta T}{\Delta T_0} = \frac{1}{1-f} \dots\dots\dots (4)$$

The ratio between temperature change with feedback (ΔT) and the temperature change without feedback (ΔT_0) can be used as the measure of feedback and referred as feedback gain, G . Therefore, feedback gain, G can be defined as the ultimate system response whether the system has intensified or dampened compared to its reference system due to addition of feedback factor.

$$G = \frac{1}{1-f} \dots\dots\dots (5)$$

Now, if the temperature changes with feedback (ΔT) is larger than temperature change without feedback (ΔT_0), the feedback factor f will be positive which will intensify the system response (here is temperature change), thus it will be termed as positive feedback. In contrast, if ΔT is smaller than ΔT_0 , the feedback factor f will be negative which will reduce temperature change, thus it is termed as negative feedback.

2.4. Climate-carbon cycle feedback system

The carbon cycle is sensitive to varying atmospheric CO₂ concentration and associated climate change. Thus, carbon cycle has great importance in all time scales for its inter-connected relation and response with climate system. In return, the climate system is affected by the atmospheric CO₂ concentration, which depends on how the land and ocean ecosystem response. This two way coupling will have impact on future climate change (Denman et al., 2007).

The present atmospheric CO₂ concentration is above its natural range compared to the last 650 000 years (Jansen et al., 2007). The atmospheric CO₂ concentration has risen sharply since the industrial revolution and in the last five decades the atmospheric CO₂ concentration has increased around 70 ppm which is undoubtedly not natural rather due to increased use of fossil fuels and land use change by human (Scripps Institution of Oceanography, 2013, Denman et al., 2007).

For being a dominant greenhouse gas, CO₂ has direct effect on climate through the greenhouse effect. Global mean temperature is predicted to increase in the coming century for increased anthropogenic CO₂ emissions in several climates model studies (Dufresne et al, 2002; Cox et al.,

2000). According to the IPCC Fourth Assessment Report (AR4), the projected global mean temperature for 21st century under a high emission scenario (A2) has been estimated in the likely range between 2-5.4 K with a best estimate of 3.4 K (Meehl et al., 2007). This increased atmospheric temperature may affect total carbon storage of land and ocean through hampering the carbon uptake processes (e.g. photosynthesis rate or reduced dissolution of CO₂ in warm sea water) or enhancing the carbon emitting processes (e.g. increased respiration) from land and ocean.

However, due to more available atmospheric CO₂, land and ocean carbon storage may enhance (e.g. CO₂ fertilization effect in land, increased dissolution of CO₂ in sea surface water) up to the saturation of the land and ocean system; afterwards it will turn to a carbon source rather than sinks. In one coupled climate-carbon model study, developed in the end of 20th century, it was shown that terrestrial biosphere turns to a carbon source for the higher emission scenario (A2) after the year 2050, however the ocean remains a carbon sink at a rate 5 Gt Cyr⁻¹ till the 21st century (Cox et al. 2000). In contrast to Cox et al. (2000), Dufresne et al. (2002), was shown that both land and ocean continue to remain a carbon sink till the 21st century.

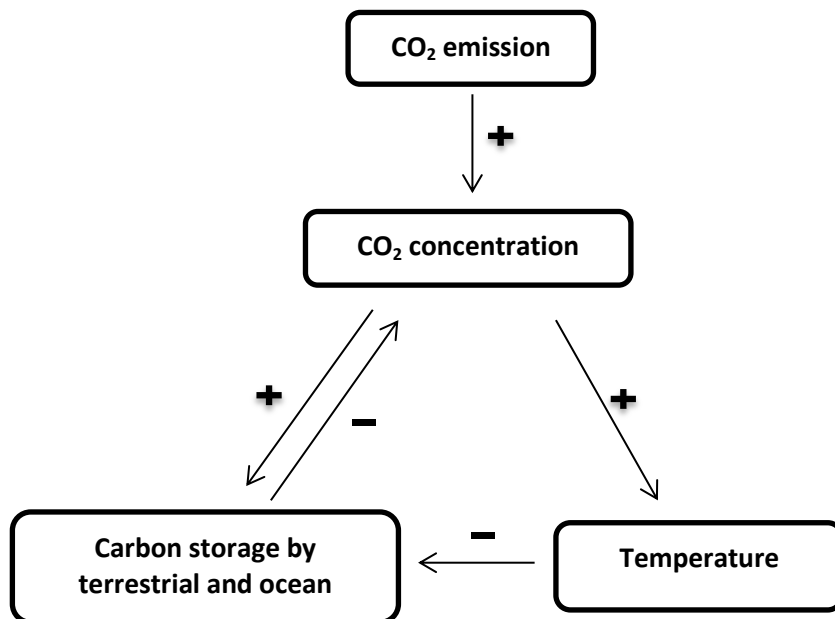


Figure 4: Positive feedback loop of climate- carbon cycle feedback system. Positive sign represents the same relative changes (increase of one component will lead to increase other or vice versa) between the components of the cycle, negative sign represents the opposite relation (increase of one component will lead to decrease other or vice versa).

In summary, increased atmospheric CO₂ concentration increases the carbon stock by land and ocean and respiration processes emit CO₂ into the atmosphere, thus decreasing the carbon storage; this increased atmospheric CO₂ alters the climate system through the greenhouse effect and in return, perturbed climate has impact on atmospheric CO₂ concentration by affecting the uptake of carbon on land and ocean which is ultimately a positive feedback loop (Fig. 4).

Several climate models have been applied in the beginning of 21st century to predict the climate change effect by the end of this century for increased anthropogenic CO₂. All the coupled climate-carbon cycle models have found more or less positive feedback between the carbon cycle and the climate system by contributing more atmospheric CO₂ (Cox et al., 2000; Dufresne et al., 2002, Friedlingstein et al., 2001; Friedlingstein et al., 2003; Friedlingstein et al., 2006). Cox et al. (2000) estimated a very large positive feedback under higher emission scenario (A2) where atmospheric CO₂ will reach 980 ppmv at the end of 2100 considering the climate change impact on the carbon cycle, but without climate change impact on carbon cycle it will be 700 ppmv. In contrast, Dufresne et al. (2002) showed three times smaller positive feedback which contributes less than 100 ppmv CO₂ into the atmosphere.

Major sensitivity components of climate-carbon cycle and their quantification:

From the above discussion and also from figure 4, the amplitude of the coupled climate-carbon cycle feedback is mainly controlled through three sensitivity parameters: the climate sensitivity to atmospheric CO₂, the carbon cycle sensitivity to CO₂ and the carbon cycle sensitivity to climate change. Therefore, the magnitude of the climate-carbon cycle feedback can be determined by estimating these sensitivity parameters.

Following Friedlingstein et al. (2003, 2006) climate sensitivity to CO₂ (in K ppm⁻¹), carbon cycle sensitivity to CO₂ (in GtC ppm⁻¹) and carbon cycle sensitivity to climate change (in GtC K⁻¹) are denoted here as α , β and γ respectively. For investigating the response of two key dominant components of the carbon cycle, carbon cycle sensitivity can be divided into land and ocean carbon cycle sensitivity; land and ocean carbon cycle sensitivity to atmospheric CO₂ are

denoted as β_L and β_o and land and ocean carbon cycle sensitivity to climate are denoted as γ_L and γ_o , respectively.

For quantifying the sensitivity components from any coupled climate-carbon cycle model, two types of simulations run named coupled and uncoupled are extensively used (Friedlingstein et al, 2003, 2006, Mikolajewicz et al., 2006). Coupled simulation represents the effect of the continuously changing atmospheric CO₂ and associated climate change on the coupled climate-carbon cycle, whereas uncoupled simulation does not represent the coupled effect of the climate-carbon cycle. In the uncoupled simulation, it has been imagined that the carbon cycle responds only to the changed atmospheric CO₂ effect, but is not affected by the associated climate change.

Climate sensitivity to CO₂, α can be estimated by analyzing how global temperature changes as a function of simulated atmospheric CO₂ from the coupled run (Friedlingstein et al, 2003).

$$\alpha = \frac{\text{Global temperature changes}}{\text{Atmospheric } CO_2 \text{ from coupled run}}$$

Carbon cycle sensitivity to CO₂, β (β_L and β_o) can be estimated from the uncoupled simulations of the model by analyzing the total carbon storage (land and ocean carbon storage) response as a function of simulated CO₂ concentration from the uncoupled simulations (Friedlingstein et al, 2006).

$$\beta (\beta_L, \beta_o) = \frac{\text{Total carbon storage (land, ocean) from uncoupled simulation}}{\text{Atmospheric } CO_2 \text{ from uncoupled run}}$$

The estimation of carbon cycle sensitivity to climate change, γ (γ_L and γ_o), can be done from the difference between coupled and uncoupled simulations of carbon flux (land and ocean) and this is influenced by both the climate change and atmospheric CO₂ concentration. Thus, climate change effect alone on carbon storage from the CO₂ induced effect needs to be isolated. To do so, first the changes in the carbon storage due to climate change can be calculated from the difference between coupled (climate change and CO₂) and uncoupled (only CO₂) simulations. Now, this carbon storage is also influenced by different level of atmospheric CO₂. Thus, the difference between this carbon storage and CO₂ induced carbon storage would be the only

climate change influenced carbon storage. CO₂ induced carbon storage can be calculated by using carbon (land, ocean) cycle sensitivity to CO₂, β (β_L and β_O) as follows:

Carbon storage due to only climate change effect = (carbon uptake on coupled run – carbon uptake on uncoupled run) - β (atmospheric CO₂ in coupled run - atmospheric CO₂ in uncoupled run) (Friedlingstein et al, 2003, Friedlingstein et al, 2006). Thus, the carbon cycle sensitivity to climate change, γ (γ_L and γ_O) can be estimated by calculating the carbon storage (land and ocean) due to climate change effect as a function of temperature changes.

$$\gamma (\gamma_L, \gamma_O) = \frac{\text{Carbon storage (land, ocean) due to climate change effect}}{\text{Temperature changes}}$$

3. Methodology

3.1. Model description

In this project, a set of global time series derived from a complex Earth system model (ESM) was used for estimating climate-carbon cycle feedbacks initiated by long-term anthropogenic climate change and CO₂ emission. This ESM was developed by a collaboration of the Max-Planck-Institute for Meteorology, Germany and the University of Wisconsin-Madison, United States in 2005, and therefore the model is named **MPI/UW ESM** (Winguth et al., 2005; Mikolajewicz et al., 2006). This complex Earth system model has been developed for studying centennial to millennial time-scale effects on the Earth system, including internal feedback mechanisms between different physical and biogeochemical parts. The model has been applied to study long-term responses of the Earth system for the past and future climate changes due to different forcing types such as insolation changes due to orbital variations (Gröger et al., 2007; Schurgers et al., 2006; Schurgers et al., 2007) and anthropogenic CO₂ emissions (Schurgers et al., 2008; Mikolajewicz et al., 2006; Winguth et al., 2005; Vizcaino et al., 2008). The model describes major physical and biogeochemical processes within the Earth system to enable the study of the consequence on the climate system of changes in the forcing. The physical part includes a coupled atmosphere-ocean general circulation model (GCM) and a three dimensional thermo-mechanical ice-sheets model. The biogeochemical part includes a marine carbon cycle model and a dynamic global vegetation model. Table 2 shows all major components within the Earth system model, the respective models used and references in details (Winguth et al., 2005; Mikolajewicz et al., 2006).

Table 2: Major components of the Earth system model (ESM), respective models and their references.

Major component of ESM	Model used	References
1. Physical part		
i. Atmospheric GCM	ECHAM3	Roekner et al.1992
ii. Oceanic GCM	LSG2	Maier-Reimer et al.1993
iii. Three dimensional thermo-mechanical ice sheet model	SICOPOLIS	Greve 1997
2. Biogeochemical part		
i. Marine carbon cycle model	HAMOCC3	Maier-Reimer 1993
ii. Dynamic global vegetation model	LPJ	Sitch et al. 2003

In the experiments that are applied in this study, the model was forced by different prescribed anthropogenic CO₂ emissions. The simulations started with a so-called spin up period, in which the model was run with constant forcing, meaning that no anthropogenic CO₂ emissions was considered. Then the model was driven by historical emissions for the period of 1750-2000 and these historical data accounted for human-induced CO₂ emissions from fossil fuel combustion, cement production and land use change. After that a 1000 year simulation has been carried out for the period of 2001-3000 where the period 2001-2100 was forced by IPCC SRES emission scenarios (Nakićenović et al., 2001) and then 2101-3000 according to an exponential decay of the emissions, during which the CO₂ concentration can stabilize (Mikolajewicz et al., 2006).

Future emissions of GHGs will be controlled by a complex dynamic process, driven by the combination of future global population growth, associated socio-economic development and technological advances. Although the prediction about the future is highly uncertain, different emission scenarios can portray possible alternative images of future world. All the IPCC SRES emission scenarios are projected, based on four main qualitative storyline (A1, A2, B1, and B2). Three distinctly different IPCC SRES emission scenarios till 21st century which were used in the model as prescribed anthropogenic CO₂ emissions are A1B, A2 and B1(Nakićenović et al., 2001).

The A1B scenario is one of the groups of A1 storyline, representing balanced use of fossil fuel. In the A1 storyline, global population will continue to increase until reaching its maximum by 2050 and decrease afterwards. Rapid economic growth and efficient technologies will take place. In consequence, socio-cultural interaction and more integrity will be observed. The A2 scenario follows a storyline that describes a more heterogeneous and fragmented world. Population growth will continue to increase, technological advances will be slowly growing and economic development will be mostly based on local orientation. The storyline which is representing B1 scenario illustrates a more united world in contrast to the other storylines. Demographic and economic development will be the same as in the A1 storyline; however there will be environmentally friendly and efficient technological advances. Therefore, A2, A1B, and B1 scenarios predict high, intermediate and low greenhouse gas emissions respectively (Nakićenović et al., 2001). However, these SRES scenarios were developed to predict centennial-scale anthropogenic CO₂ emissions and were available only till 2100. After the 21st

century a gradual decrease of anthropogenic CO₂ emissions has been assumed for stabilizing the system by applying an exponential decline with a fixed time constant of 150 years (Mikolajewicz et al., 2006).

Some assumptions were made for simplification of future emission scenarios in the model. First, nitrogen emissions from anthropogenic sources and sulphate emissions were not taken into account. In addition, the model does not include changes of dust particle despite the fact of their eventual importance for aerosol formation which might have an effect on coupling and feedback between climate and ocean biogeochemistry in future (Jickells et al. 2005). Some human-induced changes such as land use change, deforestation were not considered in the vegetation model although land use changes were included on the emission calculation; therefore LPJ estimates only potential vegetation (Mikolajewicz et al., 2006 ; Schurgers et al., 2008).

3.2. Data description

The long time series (2001 - 3000) for key parameters, describing the climate-carbon cycle system derived from the simulation result of MPI/UW ESM for each SRES (A2, A1B, B1) scenario, were available for quantifying climate-carbon cycle feedback in this project. Three different set ups were performed during simulation of the model, one common spinup was run and two other setups were run for each scenarios. The three set ups were: (i) a control run which represents a coupled run, without CO₂ emissions as forcing, resulting in dynamic CO₂ concentration around 280 ppm; (ii) a coupled run where emissions from the respective SRES scenario were applied to the model and (iii) an uncoupled run in which the climate system is not affected by the rising CO₂ concentration, but responds to a constant forcing of 280 ppm. However, the emissions affect the CO₂ concentration that interacts with the carbon cycle, thus it is possible to observe how the carbon cycle responds to only anthropogenic CO₂ emissions but not to the associated climate change. From simulations (ii) and (iii), it is possible to estimate anthropogenic climate change effect on each variable. The uncoupled model simulation results are denoted as 'nocc' (no climate change) in the figures.

The variables from MPI/UW ESM simulations which were used while calculating climate-carbon cycle feedback are: CO₂ emission in GtC (Fig. 5a); temperature changes in K for the coupled simulations (Fig. 5b); changes in atmospheric CO₂ concentration in ppm for coupled and

uncoupled simulations (Fig. 5c and 5d); ocean and terrestrial carbon storage in GtC for coupled (Fig. 5e and 5g) and uncoupled (Fig. 5f and 5h) simulations respectively. All the variables except temperature change were available as cumulative changes since pre-industrial time. The changes for each variable were derived from the difference between the simulations and the control run.

The historical data of CO₂ emission (GtC/year), CO₂ concentration (ppm), ocean carbon storage (GtC) and terrestrial carbon storage (GtC) from 1951 to 2000 were also available from the simulation of the historical period for estimating the global carbon budget in the recent past.

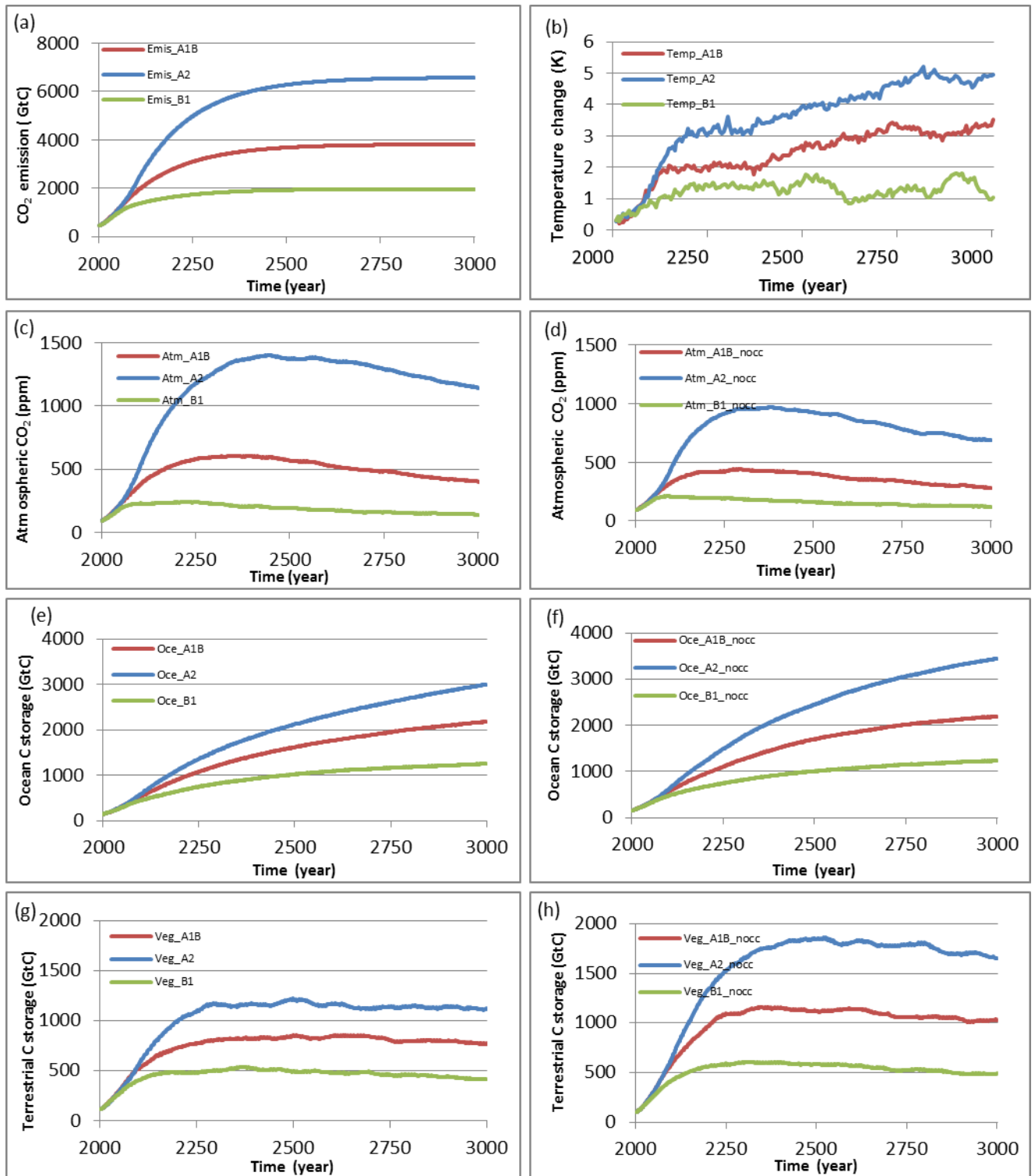


Figure 5: Time series (2001 - 3000) of component of climate-carbon cycle showing cumulative changes(except temperature and CO₂ concentration) since pre-industrial (a) CO₂ emission (b) temperature change (c), (d) atmospheric CO₂ concentration for both coupled and uncoupled ('noc') simulations respectively, (e), (f) carbon storage by ocean for coupled and uncoupled simulations respectively and (g), (h) are same as (e), (f) by terrestrial environment.

3.3. Analysis

All the calculations for analyzing the climate-carbon cycle feedback were done by using the software Microsoft Excel 2010 (Microsoft Corporation, Redmond, US). The simulation data were analyzed through different computations which were applied from similar earlier studies (Hansen et al., 1984; Friedlingstein et al., 2003; Friedlingstein et al., 2006). First of all, the global carbon budget simulated for the period 1750-2000 was computed from the time series and was compared with estimates from the IPCC report (Denman et al., 2007). The future carbon budget for the year 2100 and 3000 was estimated for three IPCC emission scenarios (A1B, A2, and B1) to investigate the difference of the carbon pools for the three alternative emission scenarios after 100 and 1000 years of simulation, respectively. Afterwards, total emitted carbon per decade, net uptake by land and ocean and subsequent atmospheric increase per decade were estimated for the period 2001 - 3000 to see the changes on centennial to millennium time-scale. The rise in CO₂ concentration will have an increasing effect on carbon uptake by land and ocean (Falkowski et al., 2000; Field et al., 1998). However, in the same time this CO₂ induced future anthropogenic climate change is believed to produce a positive feedback by reducing the efficiency of carbon uptake by terrestrial and ocean ecosystem (Cox et al., 2000, Friedlingstein et al., 2001; Cramer et al., 2001). To quantify this reduction, the difference between the coupled (climate change and CO₂) and uncoupled (only CO₂) simulation run can determine the climate change effect on carbon cycle at longer time scale. In addition, the fraction of emitted anthropogenic CO₂ emissions that exist among reservoirs (atmosphere, land and ocean) at the end of 21st century and this millennium were estimated for all the scenarios and for both coupled and uncoupled simulations.

For quantifying the climate-carbon cycle feedback (section 2.4), all the sensitivity components: α , climate sensitivity to atmospheric CO₂ (K ppm⁻¹), β , terrestrial and ocean carbon cycle sensitivity to atmospheric CO₂ (GtC ppm⁻¹) and γ , terrestrial and ocean carbon cycle sensitivity to climate (GtC K⁻¹) were estimated for the year 2100 and 3000. Therefore, the feedback factor f and gain G of the climate-carbon cycle after the perturbation of climate system due to expected future continued anthropogenic CO₂ emission were estimated by using sensitivity components (α , β and γ) for both 2100 and 3000. Moreover, a study of changes in these parameters (α , β , γ , f and G) for the period 2001 - 3000 was done for investigating how the sensitivities of the

climate carbon cycle system change on centennial to millennium time scales. Finally, a feedback analysis was carried out to detect the strength of climate-carbon cycle in terms of climate change effect alone or only atmospheric CO₂.

3.4. Method to analyze feedback

The future impact of CO₂ induced climate change on the coupled climate carbon cycle can be quantified by using the methodology of feedback analysis from Friedlingstein et al. (2003; 2006), which were based on the concept given by Hansen et al., (1984).

The atmospheric increase of CO₂, response of terrestrial and ocean carbon cycle and the associated climate change can be linearized according to Hansen et al., (1984) as the following set of equations:

$$\Delta CO_2 = \int_0^t C_{IPCC} - \Delta C_L - \Delta C_o \dots\dots\dots (6)$$

$$\Delta C_L = \beta_L \Delta CO_2 + \gamma_L \Delta T \dots\dots\dots (7)$$

$$\Delta C_o = \beta_o \Delta CO_2 + \gamma_o \Delta T \dots\dots\dots (8)$$

$$\Delta T = \alpha \Delta CO_2 + \Delta T_{ind} \dots\dots\dots (9)$$

Here,

C_{IPCC} , ΔCO_2 , ΔC_L and ΔC_o are cumulative emissions of CO₂ from IPCC SRES scenarios (GtC), atmospheric increase of CO₂ (ppm), and cumulative atmosphere-land and atmosphere-ocean CO₂ fluxes (GtC), respectively.

α , β (β_L, β_o) and γ (γ_L, γ_o) are climate sensitivity to atmospheric CO₂ (K ppm⁻¹), carbon cycle (land, ocean) sensitivity to atmospheric CO₂ (GtC ppm⁻¹) and carbon cycle (land, ocean) sensitivity to climate (GtC K⁻¹), respectively.

ΔT and ΔT_{ind} are temperature changes due to changing atmospheric CO₂ and temperature change due to other forcing (e.g. N₂O, Ozone etc).

Now, equation (6) can be rewritten by introducing ΔC_L and ΔC_O from equation (7) and (8) which is done by following the process used in feedback analysis study by Friedlingstein et al., (2003). In addition an extra conversion factor has been introduced here for maintaining the same consistency in unit. Now, atmospheric increase of CO₂, ΔCO_2 (ppm) will be expressed as ΔC_A (GtC) and the conversion factor will be expressed as δ where $\delta = 2.14 \text{ GtC ppm}^{-1}$.

Therefore,

$$\Delta CO_2 = \frac{\int_0^t C_{IPCC} - (\beta_L \Delta CO_2 + \gamma_L \Delta T) - (\beta_O \Delta CO_2 + \gamma_O \Delta T)}{\delta}$$

$$\Rightarrow \Delta C_A = \frac{\int_0^t C_{IPCC}}{(\delta + \beta_L + \beta_O)} - \frac{(\gamma_L + \gamma_O) \Delta T}{(\delta + \beta_L + \beta_O)} \dots\dots\dots (10)$$

Now, equation (9) can be introduced to equation (10),

$$\Delta C_A = \frac{\int_0^t C_{IPCC} - (\gamma_L + \gamma_O) (\alpha \Delta C_A + \Delta T_{ind})}{(\delta + \beta_L + \beta_O)}$$

$$\Rightarrow \Delta C_A = \frac{\int_0^t C_{IPCC} - (\gamma_L + \gamma_O) \Delta T_{ind}}{(\delta + \beta_L + \beta_O)} - \frac{\alpha (\gamma_L + \gamma_O) \Delta C_A}{(\delta + \beta_L + \beta_O)}$$

$$\Rightarrow \Delta C_A = \Delta C_{A_unc} + f \Delta C_A \dots\dots\dots (11)$$

Here, the first part ΔC_{A_unc} represents the change in atmospheric CO₂ concentration due to the emissions, with subtraction of the carbon uptake by land and ocean, and also any temperature-induced changes that are caused by non-CO₂ temperature effects. The second part represents the feedback, and the feedback factor, f can thus be written as a function of α , β , and δ .

To express the feedback strength with the feedback factor, f or feedback gain, G , the changes in the coupled and uncoupled simulations can be used (section 2.3):

$$\frac{\Delta C_A}{\Delta C_{A_unc}} = \frac{1}{1-f} \dots\dots\dots (12)$$

From equation (4) and (5), we know that, the ratio $1 / 1-f$ is known as feedback gain, denoted as G (Hansen et al., 1984; Roe, 2009).

Thus, from equation (12), feedback gain (G) can be written as follows:

$$G = \frac{1}{1-f} \dots\dots\dots (13)$$

Where feedback factor, $f = \frac{-\alpha (\gamma_L + \gamma_O)}{\delta + \beta_L + \beta_O} \dots\dots\dots (14)$

From the below statement given by Roe (2009) and the explanation given in the section 2.3, it is possible to interpret this unitless feedback factor and feedback gain into positive and negative feedback (depending on the range) which will provide the basis to address the ultimate impact of climate-carbon cycle feedback on climate change and on the carbon cycle.

For the condition, $-\infty < f < 0$, $G < 1$ which gives negative feedback and

$$0 < f < 1, G > 1 \text{ which gives positive feedback}$$

Now, one can quantify the feedback factor and gain by calculating the sensitivity components ($\alpha, \beta_L, \beta_O, \gamma_L$ and γ_O) of the climate-carbon cycle feedback system. The quantification of the main sensitivity components of the climate-carbon cycle feedback can be done from the coupled and uncoupled model runs by following the methodology used by Friedlingstein et al., (2006).

ΔCO_{2_cou} , ΔC_{L_cou} and ΔC_{O_cou} (ΔCO_{2_unc} , ΔC_{L_unc} and ΔC_{O_unc}) are atmospheric CO₂, land and ocean carbon storage changes for coupled (uncoupled) simulations, respectively. All units are in GtC, except atmospheric CO₂ changes, which are expressed in ppm. The effect of atmospheric CO₂ on global mean temperature change can be quantified from coupled simulation as:

$$\Delta T = \alpha \Delta CO_{2_cou} \dots\dots\dots (15)$$

So, the climate sensitivity to CO₂ at any time can be calculated from the time series described above:

$$\alpha = \frac{\Delta T}{\Delta CO_{2_cou}} \dots\dots\dots (16)$$

The response of land and ocean carbon storage due to atmospheric CO₂ change can be approximated from the uncoupled simulations as follows:

$$\Delta C_{L_unc} = \beta_L \Delta CO_{2_unc} \dots\dots\dots (17)$$

$$\Delta C_{O_unc} = \beta_O \Delta CO_{2_unc} \dots\dots\dots (18)$$

Thus, one can quantify the terrestrial and ocean carbon cycle sensitivity to atmospheric CO₂ (β_L and β_O) from the following equations by using the time series which were derived from uncoupled simulations:

$$\beta_L = \frac{\Delta C_{L_unc}}{\Delta CO_{2_unc}} \dots\dots\dots (19)$$

$$\beta_O = \frac{\Delta C_{O_unc}}{\Delta CO_{2_unc}} \dots\dots\dots (20)$$

Similarly, it is possible to define the land and ocean carbon storage changes due to atmospheric CO₂ changes from coupled simulations as follows:

$$\Delta C_{L_cou} = \beta_L \Delta CO_{2_cou} + \gamma_L \Delta T \dots\dots\dots (21)$$

$$\Delta C_{O_cou} = \beta_O \Delta CO_{2_cou} + \gamma_O \Delta T \dots\dots\dots (22)$$

Therefore, one can quantify the terrestrial and ocean carbon cycle sensitivity to climate (γ_L and γ_O) from the following equations by using the β_L and β_O from the equations (19) and (20) and the time series which were derived from coupled simulations:

$$\gamma_L = \frac{\Delta C_{L_cou} - \beta_L \Delta CO_{2_cou}}{\Delta T} \dots\dots\dots (23)$$

$$\gamma_O = \frac{\Delta C_{O_cou} - \beta_O \Delta CO_{2_cou}}{\Delta T} \dots\dots\dots (24)$$

To analyze how only the changing atmospheric CO₂ concentration or only climate change may affect the ultimate gain of the climate carbon cycle feedback system, the following methodology has been followed:

For a coupled climate-carbon cycle system equation (10) can be re-written (where total carbon cycle sensitivity to CO₂ represents, $\beta = \beta_L + \beta_O$ and similarly, total carbon cycle sensitivity to climate change, $\gamma = \gamma_L + \gamma_O$) as follows:

$$\Delta C_A = \frac{\int_0^t C_{IPCC}}{(\delta + \beta)} - \frac{\gamma \Delta T}{(\delta + \beta)} \dots\dots\dots (25)$$

$$\text{Feedback gain, } G = \frac{\Delta C_A}{\Delta C_{A_unc}} = \frac{1}{1 - f} \dots\dots\dots (26)$$

$$\text{Where feedback factor, } f = \frac{-\alpha \gamma}{\delta + \beta} \dots\dots\dots (27)$$

For climate change effect only:

Equation (25) can be rewritten as follows for no climate change (denoted as ‘nocc’) effect in the system:

$$\Delta C_{A_nocc} = \frac{\int_0^t C_{IPCC}}{(\delta + \beta)} \dots\dots\dots (28)$$

Feedback gain for climate change effect only (denoted as ‘ $G_{climate}$ ’) would be:

$$G_{climate} = \frac{\Delta C_A}{\Delta C_{A_noc}} = \frac{1}{1 - f_{climate}} \dots\dots\dots (29)$$

Therefore, the feedback factor for only climate change ($f_{climate}$) effect would be:

$$f_{climate} = 1 - \frac{\int_0^t C_{IPCC}}{\int_0^t C_{IPCC} - \gamma \Delta T} \dots\dots\dots (30)$$

For CO₂ effect only:

Equation (25) can be rewritten as follows for no CO₂ effect (denoted as ‘noc’) on climate - carbon cycle coupling system:

$$\Delta C_{A_noc} = \frac{\int_0^t C_{IPCC}}{\delta} - \frac{\gamma \Delta T}{\delta} \dots\dots\dots (31)$$

Feedback gain for CO₂ effect (denoted as ‘ G_{CO_2} ’) only would be:

$$G_{CO_2} = \frac{\Delta C_A}{\Delta C_{A_noc}} = \frac{1}{1 - f_{CO_2}} \dots\dots\dots (32)$$

Therefore, the feedback factor for only CO₂ effect (f_{CO_2}) effect would be:

$$f_{CO_2} = 1 - \frac{\delta + \beta}{\delta} \dots\dots\dots (33)$$

For multiple feedbacks in any system, feedback factors can be added to estimate the total feedback factor of that system. However, feedback gains cannot be added linearly (Roe, 2009).

Now, one can define this new feedback factor (denoted as f_{new}) by simply adding the two feedback factors ($f_{climate}, f_{CO_2}$) and in that case the new feedback gain (denoted as G_{new}) will be:

$$G_{new} = \frac{1}{1 - f_{new}} = \frac{1}{1 - f_{climate} - f_{CO_2}} \dots\dots\dots (35)$$

4. Results

By studying the global carbon budget for a certain period, it is possible to determine how much of the changed emission of atmospheric CO₂ is taken up by the terrestrial and ocean system and how much is remaining in the atmosphere. Thus, the changes in the carbon fluxes in time are possible to obtain from the estimation of how much of emitted CO₂ was used by land and ocean and how much was left in the atmosphere in past years.

4.1. Global carbon budget observed in recent past decades

Tables (3) and (4) show the global carbon budget (GtC yr⁻¹) of the last three decades as obtained from IPCC's fourth assessment report (Denman et al., 2007) and the MPI/UW ESM estimations, respectively.

Table 3: Global Carbon Budget (GtC yr⁻¹) for recent past decades estimation from IPCC (Denman et al., 2007) where (± 1) represent standard deviation for uncertainty in the estimation: CO₂ emissions rate by considering fossil fuel combustion and cement production, atmospheric CO₂ increase, total carbon uptake by ocean and land, emissions from land use change and residual terrestrial sink (2000-2005 values are not available). Positive sign representing input to the atmosphere as emissions and negative sign are losses from the atmosphere as sinks to the other components. TAR and AR4 represent the Third Assessment Report and the Fourth Assessment Report (AR4) of IPCC respectively.

IPCC	1980s (TAR)	1990s (AR4)	2000-2005 (AR4)
Emissions (fossil + cement)	5.4 ± 0.3	6.4 ± 0.4	7.2 ± 0.3
Atmospheric increase	3.3 ± 0.1	3.2 ± 0.1	4.1 ± 0.1
Net ocean-to-atmosphere flux	-1.9 ± 0.6	-1.7 ± 0.5	-2.2 ± 0.5
Net land-to-atmosphere flux	-0.2 ± 0.7	-1.4 ± 0.7	-0.9 ± 0.6
Land use change flux	1.7	1.6	N/A
Residual terrestrial sink	-1.9	-2.6	N/A

The sources of the estimations are different. The model estimations (Table 4) are based on the simulation result of this complex MPI/UW ESM whereas the IPCC estimations (Table 3) are based on the combinations of different sources of measurement where some are the result of direct measurement and some are derived indirectly. Emission rate of atmospheric CO₂ were derived from the estimation of fossil fuel and cement production data which were available up to 2003, the next two years emission rate was approximated by extrapolation of energy use data (Marland et al., 2006). Atmospheric growth rate of CO₂ was the result of direct measurement

from Mauna Loa stations (Keeling and Whorf, 2005). Ocean and land carbon fluxes with the atmosphere were approximated by using the atmospheric ratio of oxygen and nitrogen and CO₂ trend. Again, ocean to atmosphere fluxes were estimated from ocean observation and through model as well (Manning and Keeling, 2006). Thus the land to atmosphere fluxes were possible to derive by subtracting the ocean to atmosphere fluxes from the total carbon sinks. Land use change fluxes are the combination of different literature studies (Houghton et al., 2001, DeFries et al., 2002; Achard et al., 2004). The residual terrestrial carbon sink is derived from the net land to atmosphere flux and emissions from land use changes. Thus, some estimates were from direct measurement such as atmospheric CO₂ and some were derived indirectly such as residual terrestrial sink.

Table 4: Global Carbon Budget (GtC yr⁻¹) for recent past decades estimation from Model (MPI/UW ESM): CO₂ emissions rate by considering fossil fuel combustion, cement production and land use change, atmospheric CO₂ increase, total carbon uptake by ocean and land. Positive sign representing input to the atmosphere as emissions and negative sign are losses from the atmosphere as sinks to the other components.

MPI/UW ESM	1980s	1990s	2000s
Emissions (fossil + cement +land use change)	6.3	7.6	8.5
Atmospheric increase	2.8	3.2	3.2
Net ocean-to-atmosphere flux	-1.8	-1.9	-1.8
Net land-to-atmosphere flux	-1.7	-2.5	-3.5

In the IPCC estimates, CO₂ emissions from fossil fuel burning and cement production were considered and in the model, emissions from land use changes (e.g. deforestation) were also taken into account beside fossil fuel burning and cement production. However, in the IPCC estimation, emissions from land use change were estimated as flux separately, which were available for all decades except for 2000-2005 periods (Denman et al., 2007). Thus, the model estimations of CO₂ emission rate in the atmosphere are well comparable with the IPCC estimations after considering the additional emissions of CO₂ from land use change flux. Major land use changes which were contributed to CO₂ emission into the atmosphere in last two decades were deforestation in the tropical area, different agricultural practices and increased exploitation of forest resources (Denman et al., 2007).

CO₂ emission has continued to increase from 1980s to onwards up to 2000-2005 (IPCC) and 2000s (model) for both estimates due to increased contribution of CO₂ from anthropogenic sources (Table 3 and 4). Atmospheric growth rate of CO₂ has increased from 3.3 to 4.1 GtC yr⁻¹ during 2000-2005 (IPCC) and in the model estimates it has increased from 2.8 to 3.2 GtC yr⁻¹ during the period 2000s compared to 1980s. Ocean and land ecosystems are acting as sink of carbon in all time periods for both estimations. It is noticeable that, for the net land carbon uptake rate, the model estimation is the natural land flux only, on the other hand in the IPCC estimations it includes both the natural flux and land use change flux. This is because of different treatment of land use change in the two estimations, in the model it is considered as external forcing and in the IPCC estimations it is estimated as land use change flux separately. Carbon uptake rate by land has enhanced significantly from 1.7 GtC yr⁻¹ to 3.5 GtC yr⁻¹ by end decade of 20th century in the model estimations (Table 3). However, in the IPCC estimations, total land carbon uptake rate (as residual terrestrial sink) in which the natural flux and land use change flux both are included was slightly higher during the 1980s and 1990s compared to model estimations. Ocean carbon uptake rate has remained steady during last three decade in comparison to land carbon uptake rate. In the IPCC estimation, the ocean uptake rate has slightly decreased from 1980s to 1990s and then increased in the 1980s to 2000-2005 periods from 1.9 GtC yr⁻¹ to 2.2 GtC yr⁻¹ although this increase would not be significant if it accounts the uncertainty (± 0.5) of the estimations (Table 3). Ocean carbon uptake rate in the model estimation has remained steady in the range 1.8-1.9 GtC yr⁻¹ from 1980s to 2000s (Table 4). It is also noticeable for all past three decades that, almost 50% emissions of CO₂ are taken by land and ocean and other 50% are remaining in the atmosphere.

It has been cleared from both the estimations (IPCC and model) that emission of CO₂ from anthropogenic sources, atmospheric CO₂ growth rate, land carbon uptake rate were increasing, whereas the ocean carbon uptake rate remained comparatively stable, although the magnitude of carbon uptake by land and ocean were more or less the same. From the above comparison, it can be expected that this complex Earth system model is able to capture these changes which can be used to compare and explain the future global carbon budget in the next section.

4.2. Global carbon budget for the future

The carbon budget after the next 100 and 1000 years can be estimated from the long term simulations of this complex MPI/UW Earth system model for three IPCC emission scenarios (A2, A1B, B1) which were applied in the model.

4.2.1. Estimation of carbon budget for the year of 2100 and 3000

The future global carbon budget (GtC yr^{-1}) was estimated for the periods 2091-2100 and 2991-3000 from the MPI/UW ESM to investigate the changes in carbon budget for shorter time scale (centennial) and longer timescale (millennium) for three IPCC emission scenarios (A2, A1B, and B1).

Table 5: Global Carbon Budget (GtC yr^{-1}) around 2100s (2091-2100) and 3000s (2991-3000) under three different IPCC scenarios (A2, A1B, B1): CO_2 emissions rate by considering fossil fuel combustion, cement production and land use change, atmospheric CO_2 increase, total carbon uptake by ocean and land. Positive sign representing input to the atmosphere as emissions and negative sign are losses from the atmosphere as sinks to the other components.

MPI/UW ESM	2100s			3000s		
	A2	A1B	B1	A2	A1B	B1
Emissions (fossil + cement +land use change)	25.1	12.4	4.2	0.06	0.03	0.009
Atmospheric increase	13.1	5.1	-0.2	-1.50	-0.81	-0.13
Net ocean-to-atmosphere flux	-6.8	-4.7	-3.1	-0.56	-0.83	-0.61
Net land-to-atmosphere flux	-5.2	-2.6	-1.3	-1.00	-0.01	0.47

The CO_2 emission rate was high for the A2 scenario, medium for A1B and low for B1, as defined by IPCC SRES (Nakićenović et al., 2001). The CO_2 emission rate was prescribed considerably less by the end of this millennium (3000) in comparison to 21st century for the assumption made in the model set up that after 21st century, there will be exponential declines of the emissions for allowing the coupled climate-carbon cycle system to shift towards a new equilibrium point (Mikolajewicz et al., 2006). Atmospheric growth rate of CO_2 was higher for all scenarios for the period 2100s in comparison to 3000s (Table 5). This is because of the continuing increase of the emission of CO_2 in the atmosphere till the 21st century; afterwards there was a gradual decrease. This continuing decrease in emissions after 21st century and the

response of land and ocean leads to less atmospheric growth rate for the period 3000s. The net land and ocean carbon flux with atmosphere were stable with a very small increase or decrease during the period 3000s. Thus, all the carbon pools (atmosphere, land and ocean) seem like moving towards equilibrium state.

It is noticeable that atmospheric growth rate of CO₂ is negative for B1 scenario in 2100s and for all the scenarios in 3000s. The negative sign for atmospheric CO₂ growth rate means that land or ocean carbon cycle not only consuming all the additional CO₂ emission but also take up an extra amount of atmospheric CO₂ (plus the CO₂ emissions from the land or ocean when these systems are acting as source). For example, the carbon budget of B1 scenario for the period 2100s can be explained as follows: the ocean and land are taking up all the additional emitted atmospheric CO₂ (4.2 GtC yr⁻¹) plus extra 0.2 GtC yr⁻¹ atmospheric CO₂. Land and ocean continued to be a sink for atmospheric CO₂ for all the scenarios for the period 2100s. The land and ocean uptake rate for the A2 scenario were of more or less similar magnitude, which has been observed in the recent past carbon budget also (Table 3 and 4). However, for the A1B and B1 scenarios, the relative carbon uptake rate by oceans was much higher than by land.

The comparatively lower uptake rate by land and ocean for the period 3000s were because of the assumption of reduced emission rate after 21st century in order to stabilize the Earth system, which leads to the system towards a new equilibrium position. However, a decade-wise rate of change study from 2001 to 3000 has been performed in the next section to address how the changes of carbon pools in each reservoir (atmosphere, land and ocean) differ from shorter to longer time scale.

4.2.2. Changes in growth rate over time: decade by decade from 2001 to 3000

From the observation of last three decades, it is obvious that the growth rate of atmospheric CO₂ is increasing at present (Scripps Institution of Oceanography, 2013) which can be seen from recent past carbon budget as well (Table 3 and 4). As a consequence, land and ocean carbon flux will be influenced by the rise of atmospheric CO₂ which has been observed in the recent past decades as well. This increased atmospheric CO₂ is believed to affect the climate system in future (Houghton et al., 2001). In this part of the study, the rate of change of

atmospheric CO₂, land and carbon uptake has been analyzed for all emission scenarios. Short-term (inter-annual) variability was removed by taking decadal averages.

The annual increment rate of atmospheric CO₂, land and ocean systems reached a peak for all scenarios (A2, A1B, B1), afterwards there was a sharp decrease which followed a stable state with either no increase or decrease of growth rate (Fig. 6 and 7). This can be explained by the applied exponential reduction of CO₂ emission after 21st century for these simulations.

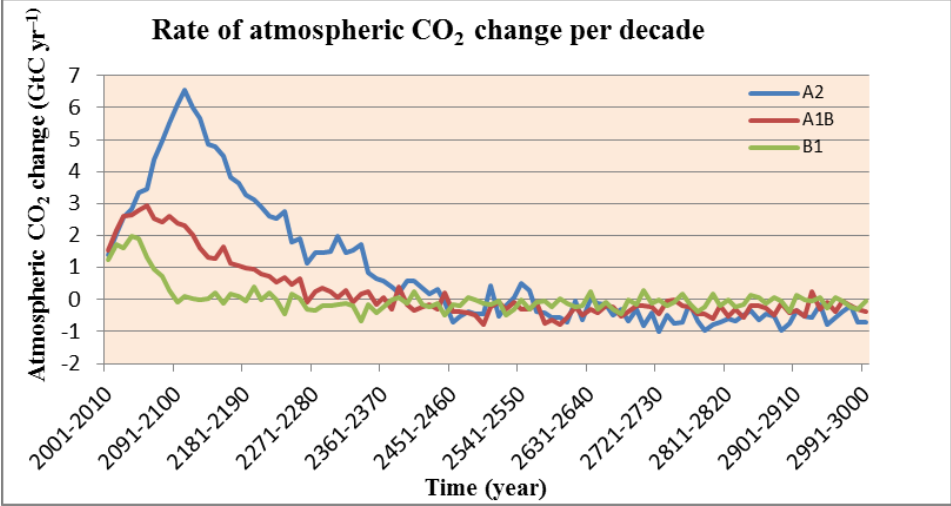


Figure 6: Atmospheric CO₂ change per decade over time period (2001- 3000).

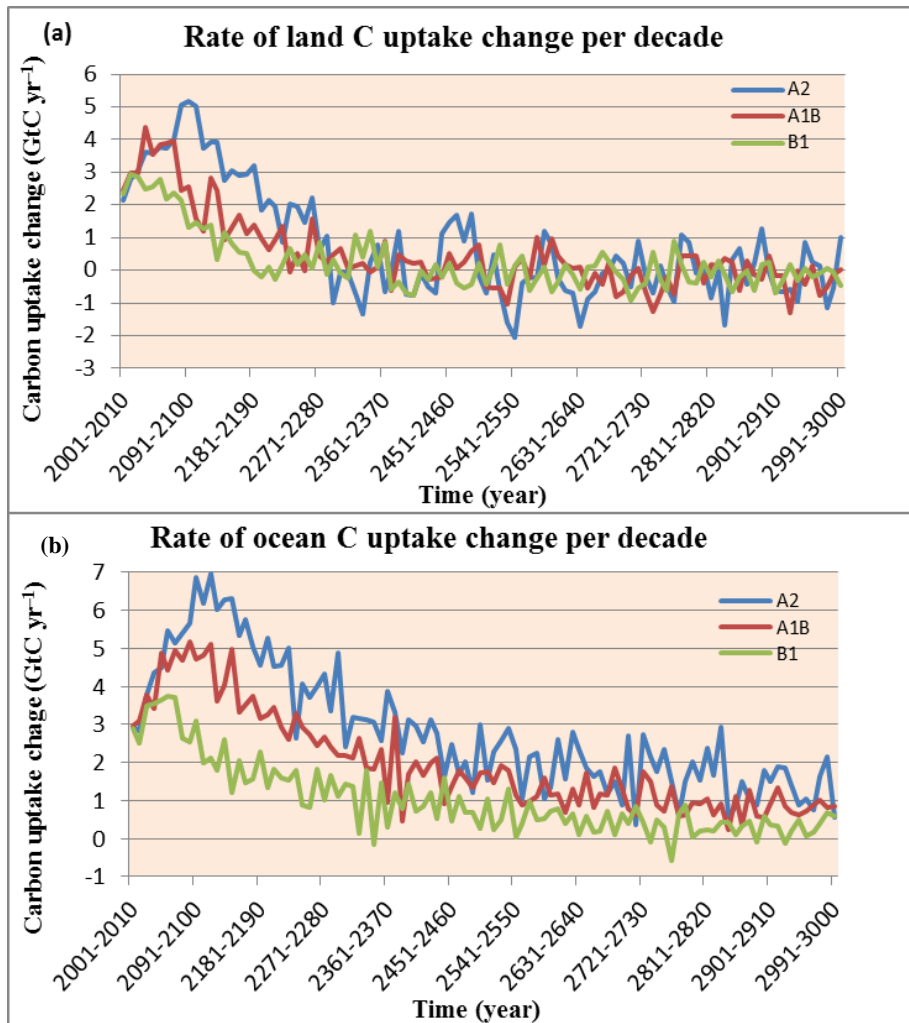


Figure 7: Changes of carbon uptake by land (a) and ocean (b) per decade over time period (2001- 3000).

The growth rate of atmospheric CO₂ reached its highest position around the period of 2101-2110 for A2 scenario. The peak for A1B and B1 scenarios reached approximately during the period 2041-2050 and 2031-2040 respectively. The peaks of atmospheric growth rate for all respective scenarios were following the same timing for reaching the peak of CO₂ emission; the peaks for CO₂ emissions for the A2, A1B and B1 scenarios were reached by the year 2100, 2050 and 2040 correspondingly (Mikolajewicz et al., 2006, Fig. 9).

Alike the CO₂ growth rate and emissions, the timing of highest increase of land and ocean carbon uptake rate were also following similar time periods. The highest uptake rates of land carbon for A2, A1B and B1 scenarios were 5.06, 4.39 and 2.92 GtCyr⁻¹ for the decades 2081-2090, 2031-2040 and 2011-2020 respectively (Fig. 7a). The ocean uptake rate showed a similar

trend (Fig. 7b). Therefore, the growth rate for the B1 scenario is going down early, then A1B and A2 scenario and this is true for all the reservoirs (atmosphere, land and ocean).

However, it is also noticeable that the decreasing trend of atmospheric growth rate had started approximately from 24th century for all the scenarios, and for the A2 scenario, this decreasing trend is stronger than for A1B and B1 scenarios (Figure 6), which can be explained by the land and ocean uptake rate. Here, terrestrial ecosystem has become either saturated or a source of carbon and ocean has continued to uptake against low emission rate of atmospheric CO₂ which result the decreased growth rate of atmospheric CO₂ (Table 4).

4.2.3. Simulated fraction of carbon emissions into air, land and ocean

In this part of the study, the analysis will be shifted from the observation of rates of change over time to the integrated changes for shorter and longer timescale. Thus, an analysis has been performed to address the relative fraction of remaining carbon in each reservoir (atmosphere, land and ocean) from the cumulative emissions of atmospheric CO₂ at the end of the 21st century and the end of the millennium, 3000, for both the coupled and uncoupled simulations from the MPI/UW ESM. Uncoupled simulations are the result of only the CO₂ induced effect on carbon cycle whereas coupled simulations are the result of coupled effect of CO₂ changes and associated climate change on carbon cycle. Thus, the result from both simulations will allow us to investigate how each of the reservoirs is influenced by only CO₂ effect (from uncoupled simulations) or by only climate change (from the difference between coupled and uncoupled simulations)

Table 6: Simulated fraction of the cumulative CO₂ emissions into air, land and ocean for the year of 2100 and 3000 under three scenarios (A2, A1B, B1). Results from both coupled (first value) and uncoupled (second within first bracket) model runs.

Scenarios	Airborne	Land-borne	Ocean-borne	Airborne	Land-borne	Ocean borne
	2100			3000		
A2	0.30 (0.26)	0.33 (0.38)	0.36 (0.36)	0.24 (0.14)	0.12 (0.14)	0.64 (0.72)
A1B	0.26 (0.22)	0.33 (0.38)	0.38 (0.38)	0.13 (0.09)	0.17 (0.19)	0.70 (0.72)
B1	0.20 (0.19)	0.38 (0.38)	0.42 (0.43)	0.08 (0.07)	0.22 (0.24)	0.70 (0.69)

The atmospheric fraction in the coupled simulation was always higher than the uncoupled simulation which is true for both the years, 2100 and 3000 and for all scenarios as well (Table 6). As described in the methodology (section 3.2), the results from the coupled simulation are obtained from the integrated effect of rising CO₂ and associated climate change, and the results from the uncoupled simulation are obtained from only rising CO₂. The higher airborne fraction in the coupled simulation is indicating that due to future anthropogenic climate change effect the airborne fraction of CO₂ will increase. The airborne fraction in 2100 was highest for the high emission scenario A2 and decreases by the year 3000 in all scenarios (Table 6). This reduction of airborne fraction by the year 3000 can be explained by investigating the partitioning of carbon between land and ocean. Land and ocean uptake of carbon was almost equal in 21st century for both simulations (coupled and uncoupled) and for all scenarios as well. However, the fraction of carbon remaining in the ocean was almost double that on the land by the end of the millennium (3000).

It is noticeable that land and ocean borne carbon fractions in the coupled simulation are either equal or less (except ocean borne fraction of B1 scenario for the year, 3000) than in the uncoupled simulations, indicating that climate change reduces the carbon uptake by land and ocean which causes the fraction of CO₂ remaining in the atmosphere to become larger. This climate change effect will be further discussed details in the next section.

4.3. Climate change effect on carbon cycle

From the above fractionation analysis of emitted carbon into air, land and ocean for both the coupled and uncoupled simulations, it has been cleared that climate change causes more of the emitted carbon to remain in the atmosphere.

Coupled simulations experience the emissions from SRES and associated climate change whereas uncoupled simulations are the result for only prescribed CO₂ from SRES emissions which is not affecting the climate system. Here, the climate is responding to preindustrial level of CO₂ (280 ppm), so there is no trend towards a warmer climate. Therefore it is possible to determine the impact of climate change alone on carbon cycle from the difference between the coupled simulations (which has climate change and CO₂ changes) and the uncoupled simulation (which has CO₂ changes alone).

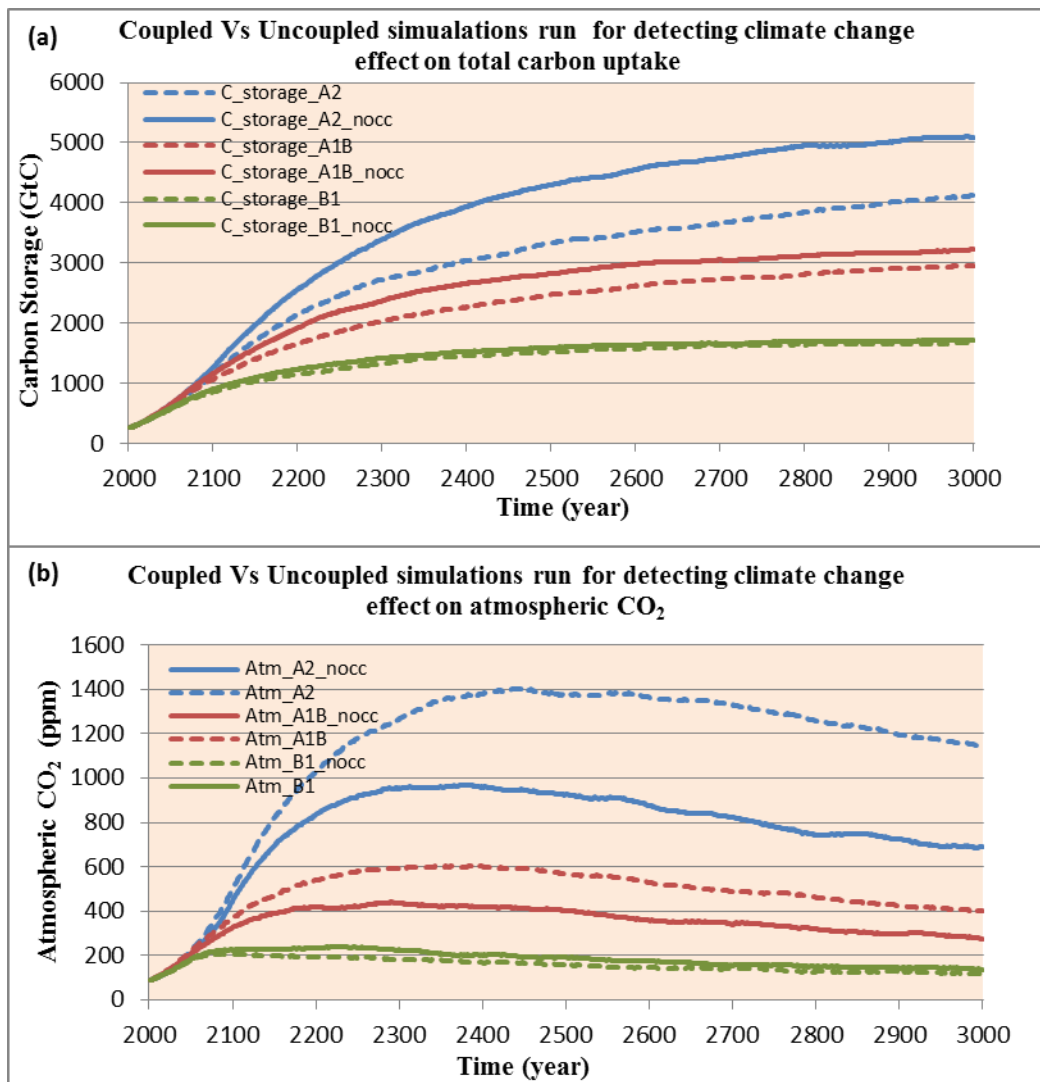


Figure 8: Comparison between coupled and uncoupled simulations for determining climate change effect on (a) total carbon storage (land and ocean) and (b) atmospheric CO₂ for all scenarios (A2, A1B, B1) from 2001 to 3000.

Coupled (climate change and CO₂) simulations resulted in lower total carbon storage in land and ocean than the uncoupled (only CO₂) simulations (Fig. 8a), showing that climate change will reduce carbon uptake in the future. Therefore, simulated atmospheric CO₂ was higher in the coupled simulation than the uncoupled simulation, indicating that there will be additional atmospheric CO₂ in future due to climate change (Fig. 8b). This is true for almost all scenarios, although the magnitude of the difference between each pair (coupled and uncoupled) for each

scenario is not the same. The reason behind this fact is the difference in magnitude among scenarios; the emissions rate of CO₂ is the highest for scenario A2, then A1B and B1. The emission rate of each scenarios increase in time although the timing of reaching their highest position is different; earlier for low emission scenario B1, then A1B and A2 (explained more in the earlier section 4.2.2). Now, these increased emissions of CO₂ may lead to the saturation effects on the land and ocean system.

Climate change lags the CO₂ changes, as the difference between coupled and uncoupled simulations tends to increase from 2001 and onwards through longer time scale (Fig. 8). This indicates that climate change happens with a short delay of increased atmospheric CO₂, thus the magnitude of climate change effect will increase in time and will affect the carbon cycle in future. The climate change effect on reduction of carbon uptake and increase of atmospheric CO₂ for longer time scale was higher for the A2 scenario, then medium for the A1B and slight effect for the B1 scenario (Fig. 8).

4.3.1. Climate change effect: Land uptake versus ocean uptake

The efficiency of carbon uptake under CO₂-induced climate change by terrestrial biosphere and ocean is very crucial for investigating how these two main reservoirs of carbon will be affected due to climate change in longer time scale. Climate change effect on land and ocean carbon uptake was analyzed from the difference between respective coupled and uncoupled simulations of land and ocean uptake from MPI/UW ESM for all scenarios.

Uncoupled simulations, which represent only the CO₂ effect, resulted in higher carbon uptake by land and ocean than coupled simulations, which represent the coupled effect of CO₂ and associated climate change (Fig. 9). Thus, it indicates that land and ocean carbon uptake will decrease due to climate change effect and this effect will be high at the end of the simulations than the beginning of the simulations. The magnitude of the climate change effect on reduction of land carbon uptake by the year 3000 was the highest for A2 scenario, medium for A1B and less for B1 (Table 7). The relative reduction of ocean carbon uptake for scenarios were showing similar results except scenario B1 in which it shows slight increase of carbon uptake rather than decrease of carbon uptake.

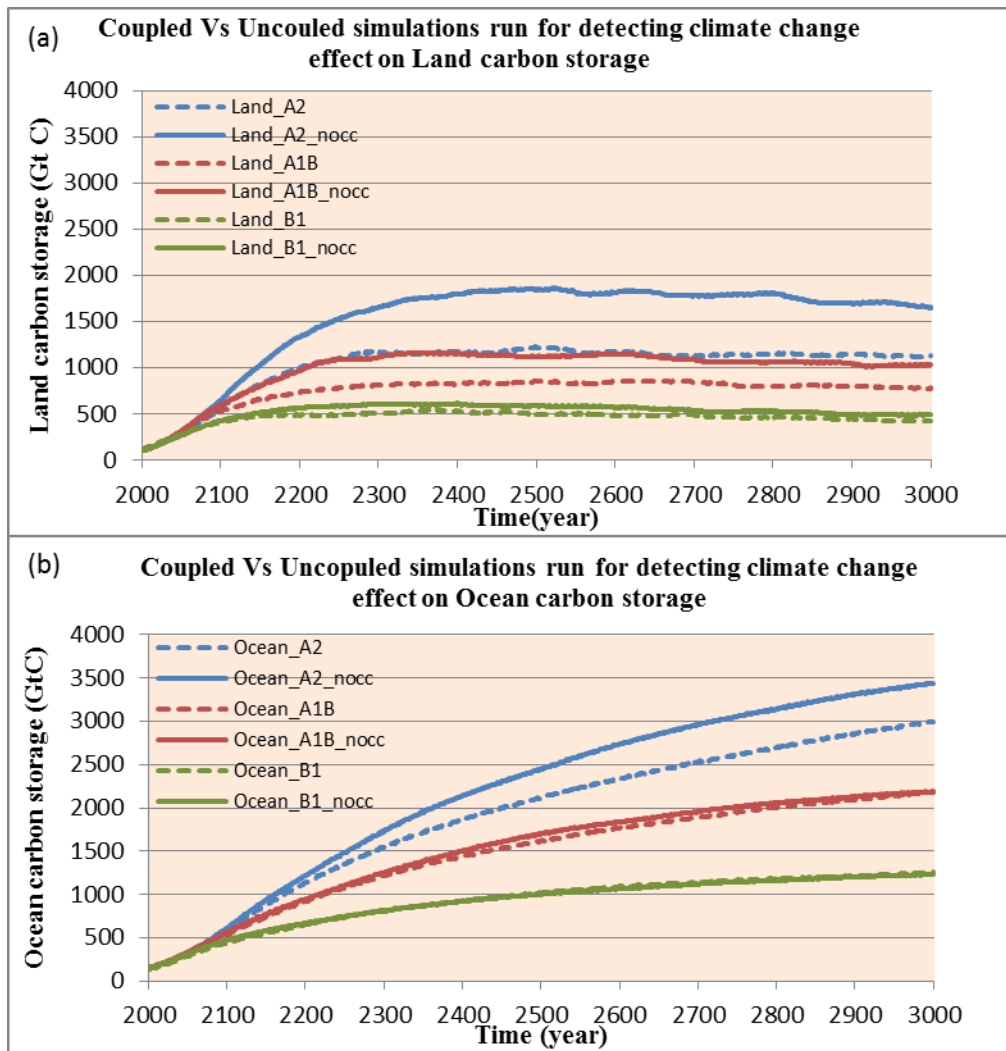


Figure 9: Comparison between coupled and uncoupled simulations run for determining climate change effect on carbon storage by (a) land and (b) ocean for all scenarios (A2, A1B, B1) from 2001 to 3000.

Table 7: Reduction of carbon uptake in percentage (%) for land and ocean due to climate change for the year of 2100 and 3000. The values represent the difference between coupled and uncoupled simulations in GtC.

Scenarios	2100		3000	
	Land	Ocean	Land	Ocean
A2	13.5	3.2	31.8	12.9
A1B	11.4	4.6	24.8	0.3
B1	4.4	4.5	14.6	-2.1

Land carbon uptake both in coupled and uncoupled simulations after the year 2300 till the end of the simulation (3000) remained stable whereas ocean showed a continuous uptake upto the year 3000 (Fig. 9a). Thus, land and ocean have different equilibration time; land has reached equilibrium state within few centuries whereas ocean has not reached its equilibrium state after 1000 years.

It is noticeable that land and ocean are not affected in the same way in terms of shorter to longer time scale due to anthropogenic climate change effect. The simulated land and ocean carbon uptake in the present time to coming few decades (2001-2050) was approximately the same with slight variation for both coupled and uncoupled simulations run and for all the scenarios as well (Fig. 9). This relatively equal distribution of carbon between land and ocean has been observed in the present time estimations also (Table 3 and 4). However, for longer time scale ocean carbon uptake was much higher than land carbon uptake. This is because, ocean continues to take up carbon till the end of the simulation whereas land uptake remained stable after the year 2300. The difference between coupled and uncoupled simulations increased in time, indicating that the reduction of carbon uptake will be enhanced due to climate change in longer time scale.

Thus, climate change impact at present and also centennial time scale (2100) on carbon storage of land and ocean has remained the same, for longer time scale (e.g. millennium) ocean carbon uptake will be affected more than the land as land is showing more stable state whereas ocean is not yet stable and continuing to take up. However, due to climate change the reduction of carbon uptake by land in comparison to ocean was affected more for both shorter (centennial) and longer (millennium) time scale (Table 7).

4.4. Climate-carbon cycle feedback analysis: short term versus long term

One of the objectives of the project was to investigate how the climate-carbon cycle feedback will be affected due to unnatural rising of atmospheric CO₂ and resultant climate change from centennial to millennium time scale. In this part of the project, the major sensitivity components of the climate-carbon cycle (which will help to calculate the gain of the feedback, which is a measure for the feedback strength) for the year 2100 and 3000 was analyzed to address the changes for shorter and longer time periods.

4.4.1. Quantifying main component sensitivities of the climate carbon cycle feedback

The major sensitivity components of climate carbon cycle feedback system are climate sensitivity to CO₂ (α), land and ocean carbon storage sensitivity to CO₂ (β_L , β_O), and land and ocean carbon storage sensitivity to climate (γ_L , γ_O). All the sensitivity components were estimated for all the scenarios which are applied in this project derived from the MPI/UW ESM for the year of 2100 and 3000, respectively (Table 8 and 9).

Table 8: Component sensitivities to the climate carbon cycle feedback: climate sensitivity to CO₂ (α), land and ocean carbon storage sensitivity to CO₂ (β_L , β_O), land and ocean carbon storage sensitivity to climate (γ_L , γ_O) for the year of 2100.

2100					
Scenarios	α (K ppm ⁻¹)	β_L (GtC ppm ⁻¹)	β_O (GtC ppm ⁻¹)	γ_L (GtC K ⁻¹)	γ_O (GtC K ⁻¹)
A2	0.0028	1.4	1.4	-113	-63
A1B	0.0035	1.8	1.7	-112	-79
B1	0.0038	2.1	2.3	-66	-74

Table 9: Component sensitivities to the climate carbon cycle feedback: climate sensitivity to CO₂ (α), land and ocean carbon storage sensitivity to CO₂ (β_L , β_O), land and ocean carbon storage sensitivity to climate (γ_L , γ_O) for the year of 3000.

3000					
Scenarios	α (K ppm ⁻¹)	β_L (GtC ppm ⁻¹)	β_O (GtC ppm ⁻¹)	γ_L (GtC K ⁻¹)	γ_O (GtC K ⁻¹)
A2	0.0043	2.4	4.9	-324	-546
A1B	0.0088	3.7	7.9	-202	-280
B1	0.0076	4.2	10.6	-153	-188

The growth rate of atmospheric CO₂ concentration in the recent decades is increasing at higher rate (Table 1). This increased atmospheric CO₂ and its well understood direct impact on climate through rise of surface air temperature is believed to enhance more in future (Foster et al., 2007). From the MPI/UW ESM, it is possible to investigate the future climate sensitivity to CO₂ for longer time scale, with the assumption of stabilization. Sensitivity of climate to CO₂, α , increased significantly between 2100 and 3000 for all scenarios (Table 8 and 9). However, it is

noticeable that for higher emission scenario, climate was showing less sensitivity, indicating that climate is less sensitive to higher atmospheric CO₂ concentration (A2) in comparison to intermediate (A1B) and lower (B1) concentration of atmospheric CO₂. Therefore, higher CO₂ emission results in lower response to the climate system. The reason for that higher emission may lead to saturation in the system fast and showing less sensitivity afterwards. This can also be explained from the equilibrium climate sensitivity which states that the same temperature rise for doubling of atmospheric CO₂. The temperature rises linearly with the doubling of atmospheric CO₂ (Scheffer et al., 2006), which means that if temperature rises 2 K for a CO₂ doubling from 200 ppm to 400 ppm, then the same temperature will rise for the doubling from 400 to 800 ppm. However, in that case climate sensitivity to CO₂, α will be less for the higher atmospheric CO₂ concentration (800 ppm) than the 400 ppm as α is estimated by temperature rise as a function of atmospheric CO₂ (section 2.4; Friedlingstein et al., 2003). Therefore, higher emissions of CO₂ result the faster CO₂ doubling in Earth system and causes less climate sensitivity to CO₂.

The behavior of the response of the carbon cycle through time evolution for continuously rising trend of atmospheric CO₂ can be detected by studying the sensitivity of land (β_L) and ocean (β_o) carbon cycle to atmospheric CO₂. Sensitivity of carbon cycle to CO₂ for both the land and ocean systems increased towards the year 3000 for all scenarios for this complex MPI/UW ESM (Table 8 and 9). This is because of the continuous uptake of carbon by land and ocean (especially by ocean), but the atmospheric CO₂ continues to decline towards the end of the millennium as the emissions of CO₂ are prescribed to drop exponentially after the 21st century till the year 3000.

The magnitude of this increased sensitivity was not the same for land and ocean. For land, it has risen almost twice and for ocean it has risen more than thrice for all respective scenarios in the year 3000 than 2100. The magnitudes of land and ocean carbon storage sensitivity for all scenarios during 21st century were roughly the same (Table 8) whereas during the year 3000, this was more than double compared to 2100 (Table 9). This indicates that in longer time scale ocean carbon uptake will be higher than the land carbon uptake. Alike α , (climate sensitivity to CO₂), β_L and β_o (land and ocean carbon storage sensitivity to CO₂) were also showing less sensitivity to higher emission scenario (A2) in comparison to intermediate (A1B) and lower (B1) emission scenarios. Less sensitivity of land carbon uptake for higher concentration of atmospheric CO₂

can be explained by the saturation of the system due to CO₂ fertilization effect (Schurgers et al., 2008). For ocean, it is because of the collapse of North Atlantic Meridional Overturning Circulation (NAMOC) for A2 scenario. As a result, the North Atlantic Deep Water (NADW) formation will be hampered due to lack of nutrient supply and less upward and downward carbon transportation. Thus, ocean will take longer time to reach its equilibrium position in comparison to A1B and B1 scenario (Mikolajewicz et al., 2006).

As discussed before in the section 2.2, increased atmospheric CO₂ has a direct impact on climate, and climate change influences the land and ocean carbon cycle. From this complex Earth system model, it is possible to investigate how the land and ocean respond over longer time periods to the impact of anthropogenic climate change. The sensitivity of land and ocean carbon storage to climate change (γ_L, γ_O) was negative, which has increased to almost double for γ_L and more than double for the year of 3000 compared to 2100 for all scenarios (Table 7 and 8). This increase of negative magnitude illustrates the fact that climate change effect will be enhanced more for longer time scale. For 21st century, γ_L and γ_O for the corresponding A2, A1B, and B1 scenarios reached to -113, -112, -66 GtC K⁻¹ and -63, -79, -74 GtC K⁻¹ respectively (Table 7). It indicates that in shorter (100 year) timescale the sensitivity of land carbon storage to changes in climate was larger than the ocean carbon storage sensitivity except for B1 scenario. However, γ_L and γ_O for longer time scale (1000 year) indicate that ocean sensitivity towards climate change was higher than the land carbon storage sensitivity to climate change for all respective scenarios (Table 8). The land and ocean carbon storage sensitivity to climate change was larger for the highest emission scenario (A2), except γ_O for the year of 2100. The complex MPI/UW ESM simulated higher global mean temperature for higher emissions of CO₂ which was the case for A2 scenario. Now, this higher temperature initiates processes such as respiration, stratification of ocean water which will result the reduced carbon storage by land and ocean. Thus, γ_L and γ_O increases with higher emission scenario, A2 in comparison to A1B and B1 (exception for γ_O during the year of 2100). However, higher emission (A2 scenario) leads to less climate sensitivity to CO₂ (α), although the global mean warming is higher for higher emission scenario, A2. The reason behind this opposite behavior is relatively poorly understood.

It may be due to the delayed response of the Earth system (land and ocean) against the increased CO₂ induced climate change (section 4.3).

4.4.2. Feedback factor and gain of the climate carbon cycle feedback

Atmospheric CO₂ has a positive impact on the climate system and on the terrestrial and ocean carbon cycle; whereas this increased CO₂ induced climate change had negative sensitivity on the terrestrial and ocean carbon cycle (Table 8 and 9). Thus, the long time series of this complex ESM showed that increased atmospheric CO₂ will tend to enhance carbon uptake by land and ocean whereas anthropogenic climate change will tend to reduce carbon uptake in future. Now, how this increased atmospheric CO₂ and climate change will be affected by the climate-carbon cycle feedback system, can be analyzed by quantifying the feedback factor and gain.

The feedback factor f is that part of the changes in the climate-carbon cycle system that is due to the perturbation in the climate system for the varying atmospheric CO₂ which can affect the land (ocean) carbon cycle in a way that the airborne fraction of atmospheric CO₂ further changes and affect the coupled climate-carbon cycle. The feedback gain G , is defined as the ultimate response of coupled climate-carbon cycle due to insertion of feedback factor (Roe 2009, section 2.3). Therefore, quantifying the feedback factor and gain (section 3.4) of climate-carbon cycle feedback allow us to compare the feedbacks in the system to a given forcing or compare the importance of different level of feedbacks through different emission scenarios.

The estimation of the feedback factor and feedback gain from the MPI/UW ESM for the year of 2100 and 3000 for all scenarios (A2, A1B and B1) were calculated from equation (14) and (13) respectively (section 3.4).

Table 10 Feedback factor f and gain G for three IPCC emissions scenarios (A2, A1B, and B1) for the year of 2100 and 3000. These terms are unitless.

Scenarios	Feedback factor , f		Feedback gain , G	
	2100	3000	2100	3000
A2	0.10	0.40	1.11	1.66
A1B	0.11	0.31	1.13	1.44
B1	0.08	0.15	1.09	1.18

As positive values of feedback factor, f , and values more than 1 of feedback gain, G , indicate positive feedback (section 3.4), the estimation of f and G of this Earth system model showed a positive feedback for both the year of 2100 and 3000 and for all scenarios (Table 10). Now, this positive feedback of climate-carbon cycle implies that due to climate change, the increased fraction of CO₂ that remained in the atmosphere will increase by producing a direct positive feedback on climate change.

Both the feedback factor and the feedback gain increased by the year 3000 compared to 2100 for the respective scenarios, thus the level of atmospheric CO₂ will increase by the end of this millennium (3000). This increased f and G of the climate-carbon cycle by the year 3000 are due to increased negative sensitivity of carbon storage towards climate change, especially higher negative ocean carbon storage sensitivity (γ_o) to climate compared to 2100 (Table 8 and 9). This negative carbon storage sensitivity causes the increased level of CO₂ that remains in the atmosphere due to the reduced carbon uptake by land and ocean. This degree of increasing pattern of the feedback factor and feedback gain for the year of 3000 follows the higher emission scenarios, meaning that f and G increases with higher emission scenario, A2, then A1B and B1 (Table 10). The reason has to be found from the relative degree of contribution of three major sensitivity components (α , β and γ) to result a higher positive feedback. The feedback factor, f will be larger, when α is larger, β is smaller and γ is negative and larger (section 3.4, Eq. 14).

During the year 3000 the carbon storage (land and ocean) sensitivity to climate (γ_L, γ_o) increases with the higher emission scenario, A2 whereas carbon storage (land and ocean) sensitivity to CO₂ (β_L, β_o) decreases with the higher emission scenario, A2 compared to other two scenarios, A1B and B1 (Table 9). So, land (ocean) carbon storage sensitivity to climate γ_L (γ_o) is more negative for higher emission scenario (A2) and so on. In contrast, carbon storage sensitivity to CO₂ β_L (β_o) is higher for lower emission scenario and so on. Therefore, the higher positive feedback of climate-carbon cycle for the longer time scale for three emission scenarios can be summarized as follows: the higher the emission, the lower the carbon storage sensitivity to CO₂ and the higher the carbon storage sensitivity to climate change. However, it

showed exception for 21st century, where f and G had reached their highest value for the intermediate emission scenario A1B. The reason can be explained by carbon storage sensitivity to climate and CO₂ both; these were higher for A1B scenario than A2 except land carbon storage sensitivity to climate (Table 8). Therefore, the f and G were slightly higher for A1B scenario than A2.

4.4.3. Comparison with other studies

Several climate model studies have investigated the coupling between climate change and carbon cycle till the 21st century by integrating IPCC high emission scenario, A2. Friedlingstein et al. (2006) have done an inter-comparison study among eleven coupled climate-carbon cycle models, named as C⁴MIP (Coupled Climate-Carbon Cycle Model Intercomparison Project). The simulations with the different models followed a similar model set up and also match with the set-up of this complex Earth system model, MPI/UW. Thus, it is possible to compare the climate-carbon cycle feedback analysis of MPI/UW for the A2 scenario and for the year 2100 with the feedback analysis of C⁴MIP.

Table 11: Comparison of climate-carbon cycle feedback analysis between MPI/UW ESM and C⁴MIP (Friedlingstein et al., 2006) for the year 2100 and for A2 scenario.

Model	α (K ppm ⁻¹)	β_L (GtC ppm ⁻¹)	β_O (GtC ppm ⁻¹)	γ_L (GtC K ⁻¹)	γ_O (GtC K ⁻¹)	Feedback factor, f
MPI/UW ESM	0.0028	1.4	1.4	-113	-63	0.10
C ⁴ MIP range	0.0038 - 0.0082	0.2 - 2.8	0.8 - 1.6	(-20) - (-177)	(-14) - (-67)	0.04 - 0.31
C ⁴ MIP average	0.0061	1.35	1.13	-79	-30	0.15

α (climate sensitivity to CO₂) of MPI/UW ESM shows lower sensitivity than C⁴MIP average and it is also not in the range of C⁴MIP. β_L (land carbon storage sensitivity to CO₂) and β_O (ocean carbon storage sensitivity to CO₂) both are showing almost similar results with C⁴MIP average which also stands in the C⁴MIP range. γ_L (land carbon storage sensitivity to climate)

and γ_o (ocean carbon storage sensitivity to climate) stays in the range of C⁴MIP, although it has much difference with the C⁴MIP average. Thus except climate sensitivity to CO₂, land and ocean carbon storage sensitivity to CO₂ and climate of this complex ESM are matching quite well with the C⁴MIP. MPI/UW ESM is simulating less climate sensitivity to CO₂ compared to all eleven coupled climate-carbon cycle models of C⁴MIP (Friedlingstein et al., 2006). The equilibrium climate sensitivity for this complex MPI/UW ESM has been estimated to 2.3 K which is comparatively less and it is slightly higher than the lower range (2.00-4.5 K) of IPCC AR4 report, 2007 (Mikolajewicz et al., 2006; Meehl et al., 2007). Finally, the feedback factor, f , for MPI/UW ESM shows slightly lower value than the C⁴MIP average, but remains within the range of C⁴MIP; indicating various magnitude of positive feedback. In summary, coupled climate carbon cycle models are able to simulate the future CO₂ induced anthropogenic climate change effect.

4.4.4. Changes in sensitivity components over time: decade by decade from 2001 to 3000

Three major sensitivity components of climate-carbon cycle feedback system are climate sensitivity to CO₂, α , land (ocean) carbon cycle sensitivity to CO₂, β_L (β_o) and land (ocean) carbon cycle sensitivity to climate change, γ_L (γ_o). All three sensitivity components are continuously changing for varying concentration of atmospheric CO₂ and resultant climate changes. In this part of the study, an average of change per decade for all the sensitivity components was analyzed for all emission scenarios from 2001 to 3000 for the MPI/UW ESM.

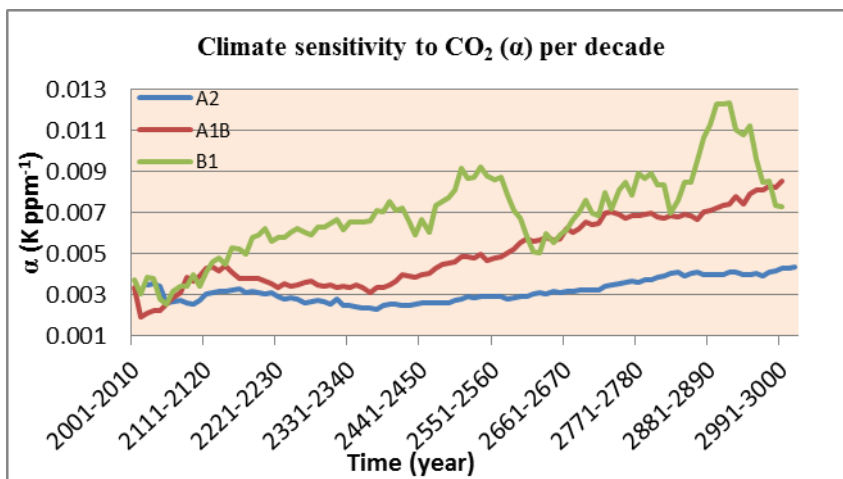


Figure 10: Change in climate sensitivity to CO₂ per decade from 2001-3000.

Climate sensitivity in terms of surface air temperature response for changing atmospheric CO₂ showed an increasing trend till the end of this millennium (3000) for all scenarios (Fig. 10). The climate sensitivity to varying atmospheric CO₂ for the higher emission scenario (A2) was lower than the other two emission scenarios A1B and B1 from the middle of 21st century to the end of the year 3000. The highest climate sensitivity to CO₂, reached 0.0043 K ppm⁻¹ and 0.0085 K ppm⁻¹ by the end decade of this millennium (2091-3000) for A2 and A1B scenarios respectively. However, for low emission scenario B1, α was showing high variability with sudden rise and fall for longer time scale; the highest sensitivity was 0.0122 K ppm⁻¹ during the decade 2891-2900. This can happen for natural variability in the Earth system for low emission of CO₂. The range of temperature changes are less against the rising of atmospheric CO₂ for low emission scenario. Thus, the noise is visible for the low emissions compared to high emissions. The climate sensitivity to CO₂ was the lowest for higher emission scenario, A2 due to saturation in the system. The climate responds to higher emission of CO₂ fast and saturated soon which afterwards shows gradual decrease of sensitivity against additional emission of CO₂ (Scheffer et al., 2006).

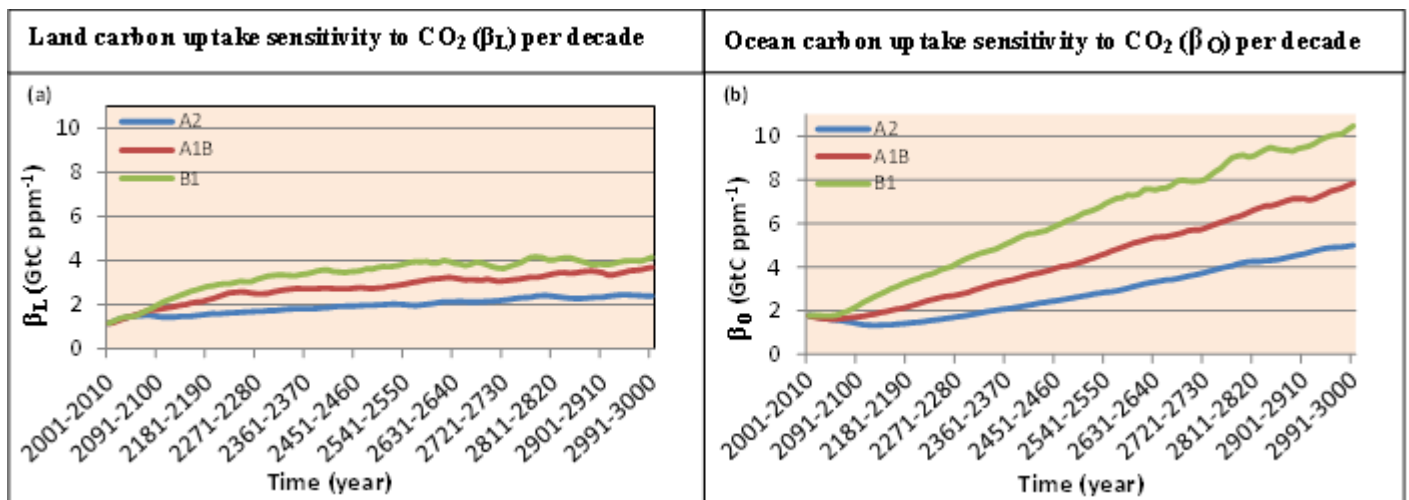


Figure 11: Change in (a) land and (b) ocean carbon uptake sensitivity to CO₂ per decade from 2001-3000.

The ocean showed higher carbon uptake sensitivity to varying CO₂ than land for three IPCC emission scenarios for longer time periods (Fig. 11). The land carbon uptake sensitivity to CO₂ (β_L) continued to increase steadily till the last decade of the year, 3000 for all scenarios. The

increased β_L for the last decade 2991-3000 was 2.4, 3.7, and 4.1 GtC ppm⁻¹ for the respective A2, A1B and B1 scenarios (Fig. 11a). Ocean uptake sensitivity to CO₂ (β_O) for all scenarios decreased slightly in the beginning of few decades, afterwards there was a sharp rise till to the last decade of the year, 3000. The increased β_O during the decade 2991-3000 was 4.9, 7.8 and 10.5 GtC ppm⁻¹ (Fig. 10b). It is noticeable from figure (11) that the rate of increase in ocean sensitivity (β_O) is much higher than the rate of increase in land carbon uptake sensitivity (β_L) as the slope of β_O is steeper than β_L . This increased rate in ocean carbon sensitivity to CO₂ became larger in time, because ocean continues to uptake the carbon till the year 3000 whereas land uptake remained stable after the 2300 to the end of the year 3000.

The relative higher carbon uptake sensitivity by land and ocean increases with lower emission scenario, meaning for low (B1), intermediate (A1B) and high (A2) emission scenarios, the sensitivity was high, intermediate and low for both the land and ocean. The reason behind this difference is that land ecosystem may become saturated soon for higher emission scenario, A2, as carbon uptake rate decreases for higher concentration of atmospheric CO₂ for this complex ESM (Schurgers et al., 2008); therefore carbon storage sensitivity shows less sensitivity for higher emission of CO₂. On the other hand, the lower carbon storage sensitivity by ocean for higher emission scenario (A2) is because of the NAMOC which was collapsed in the longer time scale simulation without any recovery till the end of 3000 (Mikolajewicz et al., 2006). As a result, there will be less downward transportation of carbon into deep ocean and the upward transportation of nutrient and high CO₂ rich deep water will also be hampered. Thus, the carbon uptake rate will be significantly reduced in case of higher emission scenario, A2. In contrast, the NAMOC was predicted a short term weakening effect in the simulations of A1B and B1 scenarios (Mikolajewicz et al., 2006).

For longer time scale, the responses of land and ocean carbon storage to varying atmospheric CO₂ are different (Fig. 11a and 11b). All scenarios during the decades around 21st century terrestrial and ocean carbon uptake were showing comparatively similar sensitivities to CO₂ (Fig. 10), but at the year 3000, the ocean uptake sensitivity is more than double in contrast to the land uptake sensitivity to CO₂. First of all, ocean carbon storage capacity is larger than land as 71% of our Earth surface is covered by ocean (NOAA, 2013); secondly, a decrease of the

terrestrial carbon uptake rate is simulated by this complex ESM after the year 2300 (Schurgers et al., 2008) which can convert the terrestrial ecosystem to a source of carbon (Fig. 6a). Finally, the continuous uptake by ocean can happen on millennium time scale due to ocean acidification which can initiate the dissolution process of calcium-rich sediments and also the transportation of carbon into the deep ocean is a comparatively slow process, thus large effects are seen at millennial rather than centennial timescales.

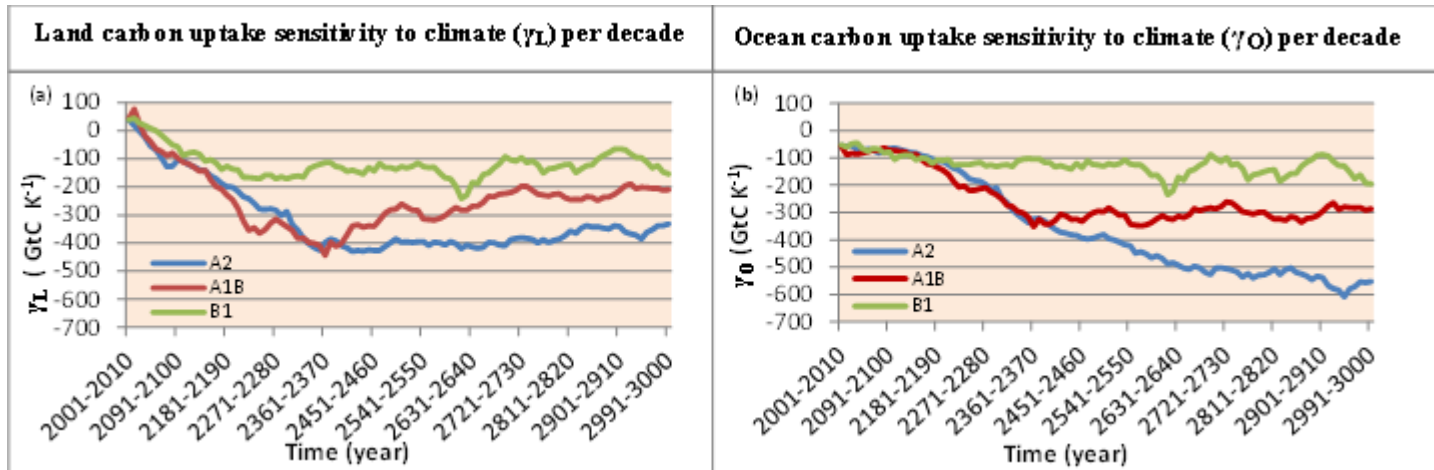


Figure 12: Change in (a) land and (b) ocean carbon uptake sensitivity to climate per decade from 2001-3000.

Land and ocean showed negative carbon storage sensitivities to climate on longer timescales, which applies to all scenarios (Fig. 12a and 12b), indicating the reduction of land and ocean carbon uptake for longer timescale due to climate change effect. The land uptake sensitivity to climate (γ_L) for A2 scenario in the beginning of two decades of 21st century was positive, afterwards this negative sensitivity increased abruptly till to -429 GtC K^{-1} for the decade 2411-2420 which was followed by a steady condition with minor variations. For A1B scenario, the change in γ_L up to the middle of 24th century was quite same with A2 scenario. The γ_L for B1 scenario was comparatively lower than the A2 and A1B scenarios.

Ocean carbon uptake sensitivity to climate (γ_O) for A2 scenario continued to increase throughout the period 2001 to 3000; the highest γ_O reached to -608 GtC K^{-1} during the decade 2941-2950. However, for A1B scenario γ_O increased from -55 GtC K^{-1} to -352 GtC K^{-1} for the

decade 2361-2370, afterwards it maintained a stable state with some variability. The γ_o for B1 scenario was less in comparison to A2 and A1B scenarios; the highest γ_o reached -234 GtC K^{-1} during the decade 2611-2620.

For longer time scale carbon storage sensitivity to climate change for both the land and ocean was larger for the higher emission scenario A2 than for A1B and B1. Higher emission of CO_2 will enhance the atmospheric CO_2 concentration which has direct impact on surface air temperature (Hansen et al., 1981) and this complex Earth system model simulates average global warming of 4.9, 3.0 and 1.3 K for the respective A2, A1B and B1 scenarios by the end of this millennium (Mikolajewicz et al., 2006). It has been addressed (section 4.3.1) that this increased global warming will significantly reduce the carbon sequestration (Fig. 9a and 9b; Table 7). Thus, these relationships can be summarized as follows: the higher the emission, the larger the climate change impact on the reduction of land and ocean carbon uptake and the higher the negative carbon storage sensitivity to climate in longer time scale.

4.4.5. Changes in feedback factor and gain over time: decade by decade from 2001 to 3000

The estimates of feedback factor f and gain for centennial (2100) and millennium (3000) scale (section 4.4.2, Table 9) indicate positive feedback of climate-carbon cycle. In this part of the study, a change in feedback factor and gain per decade have been performed to detect how these change through millennium time scale simulation with this complex ESM.

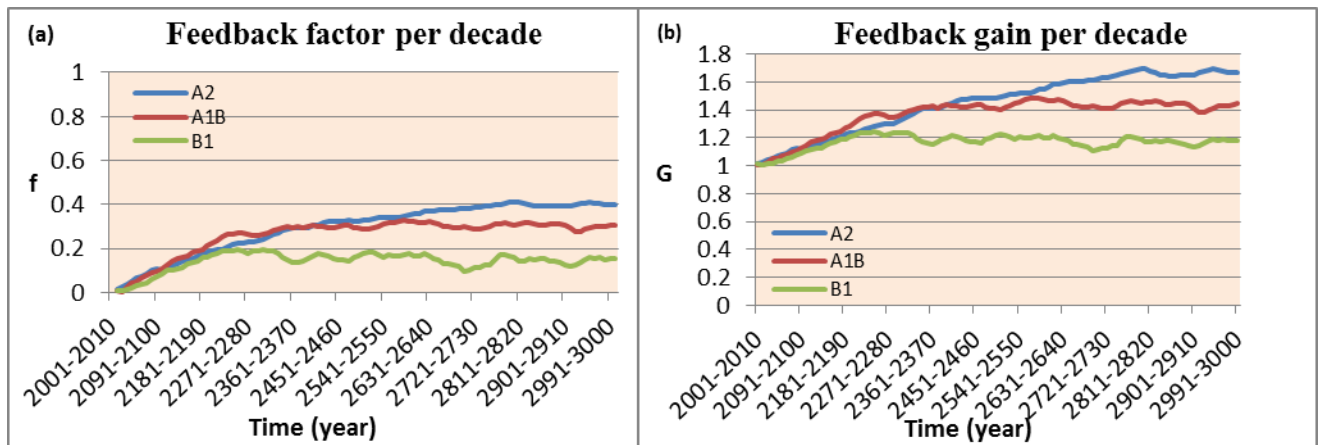


Figure 13: Changes in (a) feedback factor, f , and (b) feedback gain, G , per decade from 2001-3000.

The perturbation of the climate system due to CO₂ emissions produced a positive feedback which was showing a continuous increase throughout the period 2001-3000 for all scenarios (Fig. 13). Thus, the increased emission of anthropogenic CO₂ and associated climate change will make such changes in the coupled climate-carbon cycle system that the atmospheric CO₂ concentration will amplify more by contributing additional CO₂ into the atmosphere (Fig. 4). It is noticeable that the difference in magnitudes of feedback factor and gain, among scenarios, was less in shorter time scale in comparison to longer time scale; the difference among scenarios had started to increase from around 23rd century in the simulations. It is also noticeable that for longer timescale the magnitude of f and G were largest for higher emission scenarios. This is because of continuous higher negative carbon cycle sensitivity to climate change (Fig. 12) and lower carbon cycle sensitivity to CO₂ (Fig. 11) for high emission scenario, A2 in longer time scale. Thus, the magnitude of positive feedback will be observed more in longer time scale compared to shorter time scale for the higher climate change impact.

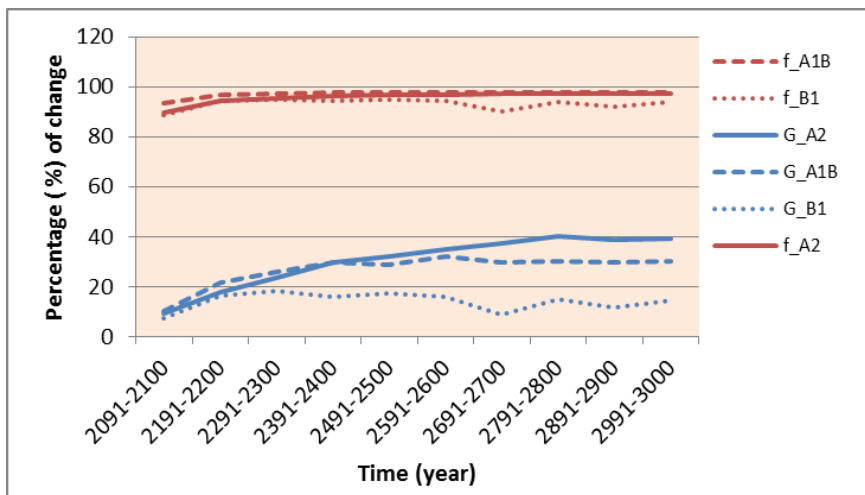


Figure 14: percentage of changes in feedback factor, f , and feedback gain, G , for all the scenarios (A2, A1B, B1) at the end of all century from 2100 to 3000 compared to the period 2001-2010.

It is noticeable that small increase in feedback factor, f , can produce higher feedback gain, G , and this can be explained by the gain curve which describes how the feedback gain changes as a function of feedback factor (Roe, 2009). The gain curve illustrates that the linear increase in feedback factor result nonlinear increase of gain. As for example, 7% increase in feedback factor produces 30% increase in feedback gain under higher emission scenarios A2 by the end of

the millennium compared to 21st century (Fig. 14). For A1B and B1 scenarios respective 4% and 5% increase of f generates 19% and 7 % increase of feedback gain. Therefore, by analyzing the feedback factor it can detect that how small forcing due to increased atmospheric CO₂ and associated anthropogenic climate change in coupled climate-carbon cycle is able to produce larger positive feedback in future.

4.5. Strength of climate change and carbon cycle separately on climate-carbon cycle feedback

In this last part of the project, the feedback factor and gain of climate-carbon cycle feedback will be analyzed by considering the disturbances due to climate change effect alone or only for changing atmospheric CO₂ on the Earth system by following the process explained in the section 3.4.

Tables (11) and (12) show the feedback factor for only climate change effect , as $f_{climate}$; for only atmospheric CO₂ effect , as f_{CO_2} ; new feedback factor, as f_{new} (which is the result of the addition of $f_{climate}$ and f_{CO_2}) and new feedback gain, as G_{new} for the year of 2100 and 3000 respectively and for three IPCC emission scenarios as well.

Table12: Feedback factors and feedback gains for three IPCC emission scenarios (A2, A1B, and B1) for the year of 2100.

Scenarios	2100			
	$f_{climate}$	f_{CO_2}	f_{new}	G_{new}
A2	0.07	-1.32	-1.24	0.45
A1B	0.15	-1.64	-1.49	0.40
B1	0.08	-2.03	-1.95	0.34

Table13: Feedback factors and feedback gain for three IPCC emission scenarios (A2, A1B, and B1) for the year of 3000.

Scenarios	3000			
	$f_{climate}$	f_{CO_2}	f_{new}	G_{new}
A2	0.19	-3.45	-3.26	0.23
A1B	0.56	-5.43	-4.87	0.17
B1	0.15	-6.92	-6.76	0.13

The positive values for feedback factor due to climate change effect alone, $f_{climate}$, on the system was indicating a positive feedback which had increased by the year 3000 compared to 2100. However, the negative values for feedback factor due to only varying atmospheric CO₂, f_{CO_2} , was indicating a negative feedback and this had also increased by the year 3000. The sign for feedback factor represents whether it will produce a positive or negative feedback; on the other hand the values represent how strong or weak the effect will be on the system.

The positive feedback produced by only climate change effect implies that due to climate change effect alone on the coupled climate-carbon cycle, there will be more remaining atmospheric CO₂ which will amplify the climate change more. However, the feedback factor for only CO₂ effect, f_{CO_2} , indicates due to increased CO₂ alone that the climate-carbon cycle will respond in a way that there will be less remaining atmospheric CO₂ which will dampen climate change more by producing a negative feedback (Table 12 and 13). Now, the new feedback factor, f_{new} , for the climate-carbon cycle can be quantified by adding these two feedback factors (section 2.3), thus it is possible to estimate the new feedback gain of climate carbon cycle feedback system.

It is also important to note here that this new feedback factor, f_{new} and gain, G_{new} are different from the before estimated feedback factor, f and gain, G as the f and G are the result of coupled effect of increased CO₂ and associated climate change on the Earth system whereas f_{new} and G_{new} are also the result of coupled climate-carbon cycle, but the increased atmospheric CO₂ and the resultant climate change were considered separately. As a result, the synergetic effect of two feedbacks (f_{CO_2} and $f_{climate}$) on each other does not account here which means that the additional effect after the interaction between climate change and carbon cycle was not captured in the new feedback factor f_{new} .

The degree of magnitude of f_{CO_2} was larger than $f_{climate}$ for both the shorter (2100) and longer (3000) timescale, indicating the negative feedback due to only atmospheric CO₂ will be dominating over the climate change effect alone till the end of this millennium. Therefore, the feedback factor, f_{new} after adding the f_{CO_2} and $f_{climate}$ was representing a negative feedback which had increased by the year 3000. Thus, the new feedback gain, G_{new} showed a negative

feedback as well for the year, 2100 and 3000. It has been noticed that G_{new} had decreased for all the respective scenarios by the year 3000 compared to 2100. This can be explained by investigating the degree of increased magnitude of $f_{climate}$ and f_{CO_2} . In contrast to f_{CO_2} , the $f_{climate}$ had increased twice during the year 3000 compared to 2100. Thus, the strength of only anthropogenic climate change is increasing more than the atmospheric CO₂ alone, although it maintained stronger effect on climate-carbon cycle by the end of the millennium.

5. Discussion

5.1. Limitation of the study

In this study, all the analysis has been done for the 21st century and for the year 3000, to study the short term (100 year) and long term (1000 year) feedback in the coupled climate-carbon cycle. However, the 21st century as short term scale may not be representative for studying centennial time scale climate carbon cycle feedback. The 21st century results represent a transient state, which is not an equilibrium state as the CO₂ forcing continues to increase during the entire period. However, such an equilibrium in the Earth system is not to be expected for the 21st century with the SRES scenarios. The millennial results have been obtained with a near constant CO₂ during the last few hundred years. This complex MPI/UW ESM shows near equilibrium state by the end of the millennium (3000) under the assumption that an exponential decline of the CO₂ emissions have been prescribed after 21st century for this ESM, so the feedback of onward centuries (e.g. 22nd, 23rd and so on) differs depending on the state of CO₂ forcing and the time to reach equilibrium state of the Earth system. Thus the feedback of 21st century and the feedback of forward centuries which are close to the equilibrium state will be different.

In the results analyzed from MPI/UW ESM, only the global temperature change effect on the Earth system due to climate carbon cycle feedback was considered here, which does not enable to show regional variability. However, not all parts of the Earth will be affected in the same way for future anthropogenic climate change, as the region of higher latitudes, especially the Arctic area, gain more temperature increase, which is usually two to three times more than the global average temperature increase (Holland and Bitz, 2003). This uneven temperature rise in the polar region is mainly caused by the feedback between snow and albedo (Holland and Bitz, 2003). In addition, climate change impact actually is the aggregation of different variables such as surface air temperature, precipitation, humidity etc. which accounts in the climate models. However, it is the only global temperature that is taken into account for analyzing climate sensitivity or climate-carbon feedback in this study. Some assumptions about future emission scenarios have not been considered in the model, which might affect the results. First of all, anthropogenic sources of nitrogen emission were not considered, which has the potential to increase in the future due to the agricultural and industrial development. Nitrogen is known as an essential nutrient for plant

productivity, thus the carbon storage efficiency by plants may be influenced by the combined effect of CO₂ fertilization and more nitrogen availability (Field, 1983). Increased nitrogen loads have great importance for higher marine productivity as well (Okin et al., 2011).

Conversely, N₂O is one of the long lived GHGs which contributes to global warming. Not only N₂O, but also other GHGs such as CH₄ are not accounted for in the model while simulating climate change. Thus the CO₂ induced global warming and the warming of both CO₂ and non CO₂ (N₂O, CH₄) GHGs would be different, which might affect the result of climate change impact on land and ocean carbon cycle. This has been shown as one of the causes of relatively higher climate sensitivity to the same level of atmospheric CO₂ in the Hadley Centre model (which accounts for both CO₂ and non CO₂ emission) and the IPSL model (which accounts only for CO₂ emissions) (Friedlingstein et al., 2003).

Secondly, land use change in the vegetation model is not included, although CO₂ emissions from land use changes are taken into account as an external forcing. Thus the vegetation model (LPJ) simulates only the potential vegetation. However, the land use change by human, especially through deforestation or by other disturbances such as forest fire, might change the vegetation pattern, influencing the land to atmosphere fluxes of CO₂. At the same time it would be difficult to predict or make any assumption about the extension of land use changes through e.g. deforestation by human after 100 years or more. The incorporation of land use change in the vegetation model would constitute an uncertainty as well.

5.3. Model sensitivity to quantify feedback

The MPI/UW ESM predicts a positive feedback between climate system and the carbon cycle for three different SRES emission scenarios (A2, A1B and B1) by the 21st century and this positive feedback became stronger by the end of the millennium (3000) compared to 2100 (Fig. 13). Two other coupled climate-carbon cycle models, whose simulations followed a similar model set up with this model, Hadley Center, UK (Cox et al., 2000) and IPSL, France (Dufresne et al., 2002) have also predicted a positive feedback for higher emission scenario A2 by the 21st century (Friedlingstein et al. 2003). Moreover, Friedlingstein et al. (2006) showed an inter-comparison of feedback analysis among eleven (including the Hadley and IPSL) similar coupled climate-carbon cycle models.

All these coupled climate-carbon cycle models result in a positive feedback factor f ; designating that higher CO₂-induced anthropogenic climate change will result in a higher fraction of emitted CO₂ remaining in the atmosphere, which will further create a positive feedback on the climate system. Although this ESM and other coupled climate-carbon cycle model studies simulate a positive feedback in the Earth system, the magnitude of this feedback varies markedly from model to model. The strongest feedback has been simulated by the Hadley model (feedback factor, $f = 0.41$) which has simulated a three times larger feedback factor for the 21st century compared to the IPSL model ($f = 0.16$) (Friedlingstein et al. 2003) and this ESM ($f = 0.10$) for the high emission scenario (A2). Two models from the C⁴MIP setup (IPSL-CM4-LOOP and CSM-1) result in almost three times smaller feedback factors than the ESM used in the current study (Friedlingstein et al. 2006, Table 3).

The feedback factor becomes larger with a higher climate sensitivity, α , and a larger negative land (ocean) carbon cycle sensitivity γ_L (γ_o) against atmospheric CO₂ induced climate change. In contrast, the feedback factor becomes smaller for the lower positive values of land (ocean) carbon cycle sensitivity β_L (β_o) to CO₂ (Eq. 14). Therefore, the difference in the magnitude of feedback among models can be explained from the difference in model sensitivity towards different components (α , β_L , β_o , γ_L and γ_o) of the coupled climate-carbon cycle.

The MPI/UW ESM shows less climate sensitivity to atmospheric CO₂ (α) in comparison to Hadley model and IPSL. The equilibrium climate sensitivity for this ESM has been estimated to 2.3 K, considering the mean temperature changes of three scenarios (A2, A1B and B1) by the end of the millennium, although this value obtained from near equilibrium state as the Earth system was not reached yet in equilibrium (Mikolajewicz et al., 2006). In the IPCC AR4 (2007), the equilibrium climate sensitivity has been estimated in the range 2.0 - 4.5 K with a best estimate of about 3K (Meehl et al., 2007). Compared to IPCC, this complex ESM has simulated less global warming for doubling of CO₂ which is slightly higher than the lower end of the range. The uncertainties of estimating the climate sensitivity arise due to other atmospheric feedbacks such as water vapor, albedo and cloud feedback (Knutti and Hegerl, 2008). Cloud feedback is considered as a major source of uncertainty for estimating climate sensitivity in climate models (Bony et al., 2006). Besides climate models, the equilibrium climate sensitivity has been

estimated based on instrumental period which indicates last 150 years and also paleoclimate data. The estimation from instrumental period seems to underestimate the climate sensitivity because of lack of proper equilibrium of the Earth system. The paleoclimate data shows similar result compared to the estimations from climate models (Knutti and Hegerl, 2008).

Land carbon uptake sensitivity to CO_2 (β_L) is similar for all three models (MPI/UW ESM, Hadley and IPSL). Ocean carbon uptake sensitivity to CO_2 (β_O) of the Hadley Centre model is comparatively lower than that of MPI/UW ESM and IPSL. However, the Hadley Centre model shows stronger negative land carbon uptake sensitivity to climate change, γ_L , because of faster turnover time of soil carbon for increased heterotrophic respiration (Cox et al., 2000; Friedlingstein et al. 2003). The climate change impact on the land carbon cycle is important for explaining the larger positive feedback simulated by Hadley model. Similarly, the relatively weaker feedback simulated by IPSL-CM4-LOOP and CSM-1 models can be explained from their small values of land carbon uptake sensitivity to climate change, γ_L (Friedlingstein et al. 2006).

This complex MPI/UW ESM simulates modest climate change impact on land carbon storage, γ_L compared to Hadley and IPSL (Table 11)). On the other hand, the ocean carbon cycle sensitivity to climate change γ_O remains low and relatively insignificant as a contributor to the magnitude of the positive feedback compared to land carbon cycle response to climate change for 100 year timescale simulations. This is because carbon storage in the ocean is affected by climate change indirectly through the change of ocean circulation and air-sea carbon exchange, and also processes such as ocean stratification, which is responsible for a lower carbon uptake from the atmosphere on short timescales (Prentice et al., 2001).

Thus, the climate change impact on the terrestrial biosphere is playing a crucial role in generating the positive feedback in the Earth system for most of the centennial timescale simulations of coupled climate-carbon cycle. Carbon storage in the terrestrial biosphere is determined through the balance of the NPP (carbon input) and heterotrophic respiration by soil micro-organisms (carbon loss). These processes are highly dependent on climate variables such as temperature and rainfall. Generally, higher temperature and moisture accelerate plant productivity, thus increasing the plant biomass as well. However, at the same time this increased

warming would enhance heterotrophic respiration, which will increase the soil turnover time and reduce the carbon stock.

Cramer et al. (2001) have studied the increased CO₂ and associated climate change impact on the terrestrial ecosystem by using six dynamic global vegetation models (DGVMs) which are forced by IPCC IS92a scenario. They have found the reduced carbon uptake by the 21st century compared to 20th century due to climate change which has increased to the range of 0.3-6.6 Gt C yr⁻¹ from 0.6-3.0 Gt C yr⁻¹ depending on DGVMs. Thus, the origins of the difference of climate change impact on land carbon cycle among models are because of use of different DGVMs and also the difference in characteristics among DGVMs. For example, Hadley and the MPI/UW ESM studied here both have used two different DGVMs, namely TRIFFID and LPJ, respectively (Dufresne et al., 2002, Mikolajewicz et al., 2006), and IPSL has fixed vegetation, not accounting for dynamic changes in the vegetation (Dufresne et al., 2002). Thus, the distribution of carbon between vegetation and soil differs among these three models. IPSL simulates more carbon in the vegetation than in the soil, Hadley simulates the opposite, more carbon stored in soil than in vegetation, and MPI/UW ESM used LPJ which is characterized to equal distribution of carbon between vegetation and soil (Dufresne et al., 2002, Table 1, Sitch et al., 2008). The effect of climate change, particularly through the impact of increased temperatures on heterotrophic respiration rates of microbial organisms, appears to outcompete the photosynthesis rate, which made the terrestrial ecosystem to become a carbon source in the Hadley Centre model.

5.3. Difference in land and ocean carbon cycle response

Land and ocean carbon cycle respond differently to increased atmospheric CO₂ and resultant climate change. Carbon storage by land and ocean tends to enhance for the increased atmospheric CO₂, especially through the CO₂ fertilization effect, whereas climate change through rising temperatures tends to reduce the land and ocean carbon storage. Similar result have been found by Dufresne et al. (2002), Friedlingstein et al. (2003) and Fung et al. (2005) under higher emission scenario A2 for the year 2100. Cox et al. (2000) has found an exceptionally strong climate change effect on land carbon cycle where the terrestrial biosphere became a carbon source for the higher emission scenario (A2) after the year 2050.

The effects of varying atmospheric CO₂ and climate change on land and ocean carbon cycle differ substantially between centennial and millennial timescales. For the 21st century (centennial), the land and ocean carbon cycle response to CO₂ are positive, and show equal distributions of carbon between land and ocean for all three scenarios (A2, A1B, B1) of this MPI/UW ESM simulations (Table 8). This equal distribution of carbon for 100 year timescales under A2 scenario has also been simulated by Dufresne et al. (2002), Friedlingstein et al. (2003); Fung et al. (2005). However, Govindasamy et al. (2005) has simulated more carbon storage in terrestrial biosphere (47 %) than the ocean (10%) for the higher emission scenario, A2. On the other hand, for the millennial timescale simulations, MPI/UW ESM does not allocate the carbon equally between land and ocean, rather ocean stores more than twice the amount of carbon stored on land. This is because the ocean continues to take up atmospheric CO₂ till the year 3000, whereas the land uptake decreased considerably after the year 2300 (Mikolajewicz et al., 2006, Schurgers et al., 2008). The climate change effects on land and ocean carbon cycle vary between centennial and millennium time scale. In the previous section (section 5.3), it has already been discussed that, for centennial time scale, the climate change impact on the land carbon cycle dominates over the impact on the ocean carbon cycle. However, for longer time scale, the ocean carbon uptake is relatively more affected by climate change than the land carbon uptake (Table 9).

The millennium time scale simulation done by MPI/UW ESM, followed by the exponential decrease in emissions of CO₂ after 21st century in order to stabilize the Earth system, showed that the land and ocean carbon uptake capacity differs substantially (Fig. 9). The highest carbon uptake rate in land and ocean follows the peak of the atmospheric CO₂ concentrations for all respective scenarios (A2, A1B and B1). After reaching the peak, land carbon uptake rate started to decrease and achieved a stable state with slight decrease after the 23rd century till the end of the millennium. In contrast to land, ocean showed a continuous uptake till the end of the millennium, although the uptake rate becomes low towards the end. After 1000 years, the land ecosystem is close to its equilibrium state, whereas ocean is still taking up carbon and has not reached its equilibrium state. Therefore, two major issues explain the difference in land and ocean carbon cycle response; one is their different equilibration time and other one is their different response towards CO₂ induced anthropogenic climate change.

6. Conclusions

The complex MPI/UW ESM has been applied here to investigate centennial to millennial timescale changes in the Earth system. It estimates a positive feedback between climate change and carbon cycle for both the centennial (2100) and millennial timescales (3000) which applies for all three IPCC SRES emission scenarios (A2, A1B and B1). This positive feedback of the coupled climate-carbon cycle implies that climate change will significantly reduce the uptake rate of carbon by land and ocean against the increased emission rate of CO₂ into the atmosphere, the remaining airborne fraction of atmospheric CO₂ will thus further increase. The magnitude of this increased airborne atmospheric CO₂ will depend on the scenario.

The following objectives (section 1.1) have been investigated to observe how the future climate and the carbon cycle will be affected by this increasing trend in positive feedback of climate carbon cycle from centennial to millennial time scale.

- 1) *To estimate and compare the future global carbon budget for shorter and longer timescales under different emission scenarios.*

For centennial timescale (2100), the annual growth rate of atmospheric CO₂ and the land and ocean carbon uptake rate will increase by following the increased emission rate of CO₂. For longer time scale (3000), all the reservoirs of carbon are approaching towards their equilibrium state with little variation due to the assumed reduction of CO₂ emission, which allows the Earth system to stabilize. Atmosphere and land reach their stable state and ocean will reach its relatively stable state (as it still shows an uptake of CO₂) by the end of the millennium.

- 2) *To analyze how the terrestrial and marine carbon storage are influenced by future anthropogenic climate change.*

Future anthropogenic climate change will reduce the carbon uptake efficiency by land and ocean. For centennial (2100) time scale, the carbon will be distributed equally between land and ocean. However, on millennial timescale, carbon storage by the ocean will be larger than by land, as the terrestrial biosphere after the 23rd century will remain stable in carbon uptake with a slight variation, whereas the ocean will continue its uptake till the end of the millennium.

- 3) *To quantify the sensitivity of climate-carbon cycle feedback in the Max-Planck-Institute / University of Wisconsin-Madison Earth System Model (MPI/UW ESM), and compare this with other studies.*

The magnitude of the coupled climate-carbon cycle feedback over time is controlled by three major sensitivity components; climate response to varying atmospheric CO₂, α ; land (ocean) carbon storage sensitivity to CO₂, β_L (β_O) and land (ocean) carbon storage sensitivity to climate change, γ_L (γ_O). Under higher emission scenario (A2) projection, this ESM has simulated a positive climate sensitivity of CO₂ and positive land (ocean) carbon cycle to CO₂, which have increased by 34% and 41% (71%) respectively for the year 3000 compared to 2100. Land (ocean) carbon cycle sensitivity to climate change γ_L (γ_O) is negative for both the shorter (2100) and longer (3000) time periods and this negative sensitivity indicates that due to higher temperature more carbon will remain in the atmosphere. This negativity has increased by 65% (85%) for the year 3000 compared to 2100. Thus, the degrees of amplification of the sensitivity components are not the same; rather it shows difference in relative increase of the sensitivity components from shorter to longer time scale. The increased negative sensitivity of land (ocean) carbon cycle to climate change for the year 3000 compared to 2100 is substantially greater than the climate and carbon cycle sensitivity to CO₂.

- 4) *To investigate whether CO₂ concentration or climate changes act as dominating factor in the climate-carbon cycle feedback system.*

The increased atmospheric CO₂ alone produce a negative feedback and climate change alone produces a positive feedback in the climate-carbon cycle for both the centennial (2100) and millennium (3000) time scale. The negative feedback due to only atmospheric CO₂ concentration on climate-carbon cycle will continue to dominate over climate change effect till the end of this millennium.

The relative magnitude of the positive feedback between carbon cycle and climate change varies depending on the scenarios. The feedback factor and gain are showing an increasing trend in time (Fig. 13) during the entire period (2001-3000) for all scenarios. The relative magnitude of feedback between scenarios changes differently for shorter to longer timescale. The feedback gain, G has increased under higher emission scenario (A2) by 9% and 39% for the last decade of

the periods 2091-2100 and 2991-3000, respectively, compared to present time, 2001-2010. For the intermediate (A1B) and low (B1) emission scenarios, the feedback gain has increased by 10% and 7% respectively for centennial (2100) time scale which were further increased to 30% and 14% for the millennial timescale (3000). Thus, for shorter to longer time scale it is not only the higher CO₂ forcing (A2) but also the intermediate scenario A1B that produce a strong positive climate-carbon cycle feedback.

In summary, the increased atmospheric CO₂ alone intends to increase the carbon storage and climate change reduces the carbon storage. Climate change will thus partially offset the total carbon storage, which will have a positive feedback on the climate system. Therefore, in longer time scale climate change impact will play crucial role on producing the larger magnitude of positive feedback in the Earth System. An important aspect revealed from the millennium timescale simulations of this complex MPI/UW ESM is that the Earth system can respond strongly towards climate change when it reaches an equilibrium state. On the other hand, the result from other simulations which are based on 21st century does not reveal the full extent of feedback as Earth system has not reached in its equilibrium state. Therefore, longer timescale simulation (millennium or more) is necessary to study the full extent of climate-carbon cycle feedback which may help the policy makers to implement the rules and regulations on CO₂ emissions.

Acknowledgements

I would like to express my sincere gratitude to my supervisor Guy Schurgers for providing the global long time series for quantifying climate-carbon feedback and for his time, quick feedback, and guidance during the entire period of this project.

References

- Achard, F., Eva, H.D., Mayaux, P., Stibig, H-J., Belward, A., (2004). Improved estimates of net carbon emissions from land cover change in the tropics for the 1990s, *Global Biogeochemical Cycles*, 18:GB2008.
- Archer, D., Martin, P., Buffett, B., Brovkin, V., Rahmstorf, S., Ganopolski, A., (2004). The importance of ocean temperature to global biogeochemistry”, *Earth and Planetary Science Letters*, 222:333-348.
- Archer, D., (2005). Fate of fossil fuel CO₂ in geologic time, *Journal of Geophysical Research*, 110: C09S05.
- Archer, D., and Brovkin, V., (2008). The millennial atmospheric lifetime of anthropogenic CO₂, *Climatic Change*, 90: 283-297.
- Arrhenius, S., (1896). On the influence of carbonic acid in the air upon the temperature on the ground, *Philosophical Magazine*, 41:237-276.
- Bice, D., (2012). Overview of the Carbon Cycle from the Systems Perspective, retrieved from <https://www.e-education.psu.edu/earth103/node/692> , 02-05-2013.
- Bates, J.R., (2007). Some consideration of the concept of climate feedback, *Quarterly Journal of the Royal Meteorological Society*, 133:545-560.
- Berner, R.A., (2003). The long-term carbon cycle, fossil fuels and atmospheric composition, *Nature*, 426: 323-326.
- Bindoff, N.L., Willebrand, J., Artale, V., Cazenave, A., Gregory, J., Gulev, S., Hanawa, K., Le Quéré, C., Levitus, S., Nojiri, Y., Shum, C.K., Talley, L.D., Unnikrishnan, A., (2007). Observations: Oceanic Climate Change and Sea Level. In: *Climate Change 2007: The Physical Science Basis. Contribution of Working Group I to the Fourth Assessment Report of the Intergovernmental Panel on Climate Change* [Solomon, S., D. Qin, M. Manning, Z. Chen, M. Marquis, K.B. Averyt, M. Tignor and H.L. Miller (eds.)]. Cambridge University Press, Cambridge, United Kingdom and New York, NY, USA.

- Bond-Lamberty, B., Wang, C., Gower, S.T., (2004). A global relationship between the heterotrophic and autotrophic components of soil respiration?, *Global Change Biology*, 10: 1756-1766.
- Bopp, L., Monfray, P., Aumont, O., Dufresne, J.-L., Treut, H.L., Madec, G., Terray, L., Orr, J. (2001). Potential impact of climate change on marine export production, *Global Biogeochemical Cycles*, 15:81-99.
- Caldeira, K. and Wickett M. E. (2003). Anthropogenic carbon and ocean pH, *Nature*, 425:365.
- Cao, M. and Woodward, F.I., (1998). Dynamic responses of terrestrial ecosystem carbon cycling to global climate change, *Nature*, 393:249-252.
- Cox, P. M., Betts, R. A., Jones, C. D., Spall, S. A., Totterdell, I. J., (2000). Acceleration of global warming due to carbon cycle feedbacks in a coupled climate model, *Nature*, 408:184-187.
- Cramer, W., Bondeau, A., Woodward, F. I., Prentice, I. C., Betts, R. A., Brovkin, V., Cox, P. M., Fisher, V., Foley, J., Friend, A. D., Kucharik, C., Lomas, M. R., Ramankutty, N., Sitch, S., Smith, B., White, A. Young Molling C., (2001). Global response of terrestrial ecosystems structure and function to CO₂ and climate change: results from six dynamic global vegetation models, *Global Change Biology*, 7:357-374.
- Davidson, E.A. and Janssens, I.A., (2006). Temperature sensitivity of soil carbon decomposition and feedbacks to climate change, *Nature*, 440:165-173.
- DeFries, R.S., Houghton, R.A., Hansen, M.C., Field, C.B., Skole, D., Townshend, J., (2002). Carbon emissions from tropical deforestation and regrowth based on satellite observations for the 1980s and 1990s. *Proceedings of the National Academy of Sciences U.S.A.*, 99(22):14256-14261.
- Denman, K.L., Brasseur, G., Chidthaisong, A., Ciais, P., Cox, P.M., Dickinson, R.E., Hauglustaine, D., Heinze, C., Holland, E., Jacob, D., Lohmann, U., Ramachandran, S., Silva Dias, P.L. da., Wofsy, S.C., Zhang, X., (2007). Couplings Between Changes in the Climate System and Biogeochemistry. In: *Climate Change 2007: The Physical Science Basis. Contribution of Working Group I to the Fourth Assessment Report of the Intergovernmental Panel on Climate Change* [Solomon, S., D. Qin, M. Manning, Z. Chen, M. Marquis, K.B. Averyt, M. Tignor and H.L. Miller (eds.)]. Cambridge University Press, Cambridge, United Kingdom and New York, NY, USA.
- DeLucia, E. H., Hamilton, J.G., Naidu, S. L., Thomas, R. B., Andrews, J. A., Finzi, A., Lavine, M., Matamala, R., Mohan, J. E., Hendrey, G. R., Schlesinger, W. H., (1999). Net Primary Production of a Forest Ecosystem with Experimental CO₂ Enrichment, *Science*, 284:1177-1179.

- Dufresne, J.-L., Friedlingstein, P., Berthelot, M., Bopp, L., Ciais, P., Fairhead, L., Le Treut, H., Monfray, P., (2002). On the magnitude of positive feedback between future climate change and the carbon cycle, *Geophysical Research Letters*, 29: 10.1029/2001GL013777.
- Eby, M., Zickfeld, K., Montenegro, A., Archer, D., Meissner, K.J., Weaver, A.J., (2009). Lifetime of anthropogenic climate change: Millennial time-scales of potential CO₂ and surface temperature perturbations, *Journal of Climate*, 22:2501- 2511.
- Falkowski, P., Scholes, R. J., Boyle, E., Canadell, J., Canfield, D., Elser, J. , Gruber, N., Hibbard, K., Hoegberg, P. , Linder, S., Mackenzie, F. T., Moore III, B., Pedersen, T., Rosenthal, Y. , Seitzinger , S., Smetacek, V., Steffen, W. , (2000). The Global Carbon Cycle: A Test of Our Knowledge of Earth as a System, *Science*, 290: 291-296.
- Feely, R.A., Sabine , C.L., Lee, C., Berelson ,W., Kleypas , J., Fabry, V.J., Millero , F.J.,(2004). Impact of Anthropogenic CO₂ on the CaCO₃ System in the Oceans, *Science*, 305: 362-366.
- Field, C., (1983). Allocating Leaf Nitrogen for the Maximization of Carbon Gain: Leaf Age as a Control on the Allocation Program, *Oecologia*, 56: 341-347.
- Field, C. B., Behrenfield, M. J., Randerson, J. T., Falkowski, P., (1998). Primary production of the biosphere: integrating terrestrial and oceanic components, *Science*, 281: 237-240.
- Forster, P., Ramaswamy, V., Artaxo, P. , Berntsen, T., Betts, R., Fahey, D.W. , Haywood, J., Lean, J., Lowe, D.C., Myhre, G., Nganga, J., Prinn, R. , Raga, G., Schulz, M., Dorland, R. V. ,(2007). Changes in Atmospheric Constituents and in Radiative Forcing. In: Climate Change 2007: The Physical Science Basis. Contribution of Working Group I to the Fourth Assessment Report of the Intergovernmental Panel on Climate Change [Solomon, S., D. Qin, M. Manning, Z. Chen, M. Marquis, K.B. Averyt, M. Tignor and H.L. Miller (eds.)]. Cambridge University Press, Cambridge, United Kingdom and New York, NY, USA.
- Friedlingstein, P., Bopp, L., Ciais, P., Dufresne, J.-L., Fairhead, L., LeTreut, H., Monfray, P., Orr, J., (2001). Positive feedback between future climate change and the carbon cycle, *Geophysical Research Letters*, 28 (8):1543-1546.
- Friedlingstein, P., Dufresne, J.-L., Cox, P.M., Rayner, P., (2003). How positive is the feedback between climate change and carbon? *Tellus*, 55B:692-700.
- Friedlingstein, P., Cox, P., Betts, R., Bopp, L., Von Bloh, W., Brovkin, V., Cadule, P., Doney, S., Eby, M., Fung, I., Bala, G., John, J., Jones, C., Joos, F., Kato, T., Kawamiya, M., Knorr, W., Lindsay, K., Matthews, H., Raddatz, T., Rayner, P., Reick, C., Roeckner, E., Schnitzler, K.-G., Schnur, R., Strassmann, K., Weaver, A., Yoshikawa, C., Zeng, N., (2006). Climate-carbon cycle feedback analysis: results from the C⁴MIP model intercomparison, *Journal of Climate*, 19(14):3337-3353.

- Fung, I. Y., Doney, S. C., Lindsay, K., and John, J., (2005). Evolution of carbon sinks in a changing climate, *Proceedings of the National Academy of Sciences U.S.A.*, 102(32):11201-11206.
- Greve, R., (1997). Application of a polythermal three-dimensional ice sheet model to the Greenland Ice Sheet: response to steady-state and transient climate scenarios, *Journal of Climate*, 10:901-918.
- Goodwin, P., Williams, R.G., Ridgwell, A., Follows, M.J., (2009). Climate sensitivity to the carbon cycle by past and future changes in ocean chemistry, *Nature Geoscience*, 2: 145-150.
- Govindasamy, B., Thompson, S., Mirin, A., Wickett, M., Caldeira, K., Delire, C., (2005). Increase of Carbon Cycle Feedback with Climate Sensitivity: Results from a coupled Climate and Carbon Cycle Model, *Tellus*, 57B: 153-163.
- Gröger, M., Maier-Reimer, E., Mikolajewicz, U., Schurgers, G., Vizcaíno, M., Winguth, A., (2007). Changes in the hydrological cycle, ocean circulation, and carbon/ nutrient cycling during the last interglacial and glacial transition, *Paleoceanography*, 22: PA4205.
- Hansen, J., Johnson, D., Lacis, A., Lebedeff, S., Lee, P., Rind, D., Russell, G., (1981). Climate Impact of Increasing Atmospheric Carbon Dioxide, *Science*, 213(4511): 957-966.
- Hansen, J., Lacis, A., Rind, D., Russell, G., Stone, P., Fung, I., Ruedy, R., Lerner, J., (1984). Climate sensitivity: Analysis of feedback mechanisms, *In Climate Processes and Climate Sensitivity, AGU Geophysical Monograph 29, Maurice Ewing*, 5: 130-163.
- Heinze, C., Maier-Reimer, E. and Winn, K., (1991). Glacial pCO₂ reduction by the World Ocean: experiments with the Hamburg carbon cycle model, *Paleoceanography*, 6: 395-430.
- Holland, M.M. and Bitz, C.M., (2003). Polar amplification of climate change in coupled models, *Climate Dynamics*, 21:221-232.
- Houghton, J.T., Ding, Y., Griggs, D.J., Noguer, M., Van Der Linden, P.J., Dai, X., Maskell, K., Johnson, C.A., (2001). *Climate change 2001: the scientific basis*. Cambridge University Press, Cambridge.
- IPCC, (2000). *Land use, land use change and forestry. A special report of the IPCC*. Cambridge, UK, Cambridge University Press.
- Jansen, E., Overpeck, J., Briffa, K.R., Duplessy, J.-C., Joos, F., Masson-Delmotte, V., Olago, D., Otto-Bliesner, B., Peltier, W.R., Rahmstorf, S., Ramesh, R., Raynaud, D., Rind, D., Solomina, O., Villalba, R., Zhang, D., (2007). Palaeoclimate. In: *Climate Change 2007: The Physical Science Basis. Contribution of Working Group I to the Fourth*

Assessment Report of the Intergovernmental Panel on Climate Change [Solomon, S., D. Qin, M. Manning, Z. Chen, M. Marquis, K.B. Averyt, M. Tignor and H.L. Miller (eds.)]. Cambridge University Press, Cambridge, United Kingdom and New York, NY, USA.

- Jickells, T.D., An, Z.S., Andersen, K.K., Baker, A. R., Bergametti, G., Brooks, N., Cao, J. J. , Boyd, P. W., Duce, R. A., Hunter, K. A., Kawahata, H., Kubilay, N., laRoche, J., Liss, P. S., Mahowald, N., Prospero, J. M., Ridgwell, A. J., Tegen, I., Torres, R., (2005). Global iron connections between desert dust, ocean biogeochemistry and climate. *Science*, 308(5718):67-71.
- Joos, F., Plattner, G. K., Stocker, T. F., Marchal, O., Schmittner, A., (1999). Global warming and marine carbon cycle feedbacks on future atmospheric CO₂, *Science*, 284: 464-467.
- Joos, F., Prentice, I.C., Sitch, S., Meyer, R., Hooss, G., Plattner, G.K., Gerber, S., Hasselmann, K., (2001). Global warming feedbacks on terrestrial carbon uptake under the Intergovernmental Panel on Climate Change IPCC emission scenarios, *Global Biogeochemical Cycles*, 15(4):891-907.
- Keeling, C., (1960). The concentration and isotopic abundance of carbon dioxide in the atmosphere, *Tellus*, 12: 200-203.
- Keeling, C., (1973). Industrial production of carbon dioxide from fossil fuels and limestone, *Tellus*, 25:174-198.
- Keeling, C.D. and Whorf, T.P., (2005), Atmospheric CO₂ records from sites in the SIO air sampling network. In: Trends: A Compendium of Data on Global Change. Carbon Dioxide Information Analysis Center, Oak Ridge National Laboratory, U.S. Department of Energy, Oak Ridge, TN, <http://cdiac.ornl.gov/trends/co2/sio-keel.html>.
- King, A.W., Post, W.M., Wullschlegel, S.D., (1997). The potential response of terrestrial carbon storage to changes in climate and atmospheric CO₂, *Climatic Change*, 35: 199-227.
- Knorr, W., Prentice, I.C., House, J.I., Holland, E.A., (2005). Long-term sensitivity of soil carbon turnover to warming", *Nature*, 433:298-301.
- Knutti, R. and Hegerl, G.C., (2008). The equilibrium sensitivity of the Earth's temperature to radiation changes, *Nature Geoscience*, 01: 735-743.
- Lal, R., (2004). Soil carbon sequestration to mitigate climate change, *Geoderma*, 123: 1-22.
- Lenton, T. M., and Britton, C., (2006). Enhanced carbonate and silicate weathering accelerates recovery from fossil fuel CO₂ perturbations, *Global Biogeochemical Cycles*, 20: GB3009.

- Le Treut, H., R. Somerville, U. Cubasch, Y. Ding, C. Mauritzen, A. Mokssit, T. Peterson and M. Prather, (2007): Historical Overview of Climate Change. In: *Climate Change 2007: The Physical Science Basis. Contribution of Working Group I to the Fourth Assessment Report of the Intergovernmental Panel on Climate Change* [Solomon, S., D. Qin, M. Manning, Z. Chen, M. Marquis, K.B. Averyt, M. Tignor and H.L. Miller (eds.)]. Cambridge University Press, Cambridge, United Kingdom and New York, NY, USA.
- Maier-Reimer, E., (1993). Geochemical cycles in an ocean general circulation model. Preindustrial tracer distributions, *Global Biogeochemical Cycles*, 7:645-677.
- Maier-Reimer, E., Mikolajewicz, U., Hasselmann, K., (1993). Mean circulation of the Hamburg LSG OGCM and its sensitivity to the thermohaline surface forcing, *Journal of Physical Oceanography*, 23:731-757.
- Marland, G., Boden, T.A., Andres, R.J., (2006). Global, regional, and national CO₂ emissions. In: *Trends: A Compendium of Data on Global Change. Carbon Dioxide Information Analysis Center, Oak Ridge National Laboratory, U.S. Department of Energy, Oak Ridge, TN*, <http://cdiac.ornl.gov/>.
- Meehl, G.A., Stocker, T.F., Collins, W.D., Friedlingstein, P., Gaye, A.T., Gregory, J.M., Kitoh, A., Knutti, R., Murphy, J.M., Noda, A., Raper, S.C.B., Watterson, I.G., Weaver, A.J., Zhao, Z.-C., (2007). Global Climate Projections. In: *Climate Change 2007: The Physical Science Basis. Contribution of Working Group I to the Fourth Assessment Report of the Intergovernmental Panel on Climate Change* [Solomon, S., D. Qin, M. Manning, Z. Chen, M. Marquis, K.B. Averyt, M. Tignor and H.L. Miller (eds.)]. Cambridge University Press, Cambridge, United Kingdom and New York, NY, USA.
- Mikolajewicz, U., Gröger, M., Maier-Reimer, E., Schurgers, G., Vizcaíno, M., Winguth, A., (2006). Long-term effects of anthropogenic CO₂ emissions simulated with a complex Earth system model, *Climate Dynamics*, 28:599-633.
- Nakićenović, N., Alcamo, J., Davis, G., DeVries, B., Fenhann, J., Gaffin, S., Gregory, K., Grubler, A., Jung, T.Y., Kram, T., Lebre La Rovere, E., Michaelis, L., Mori, S., Morita, T., Pepper, W., Pitcher, H., Price, L., Riahi, K., Roehrl, A., Rogner, H., Sankovski, A., Schlesinger, M., Shukla, P., Smith, S., Swart, R., Van Rooijen, S., Victor, N., Dadi, Z., (2001). Special report on emissions scenarios. In: *A special report of Working Group III of the Intergovernmental Panel on Climate Change*. Cambridge University Press, Cambridge.
- NASA, (2011). The slow carbon cycle, retrieved from http://earthobservatory.nasa.gov/Features/CarbonCycle/carbon_cycle2001.pdf , 21-04-2013.
- Orr, J. C., Fabry, V. J., Aumont, O., Bopp, L., Doney, S. C., Feely, R. A., Gnanadesikan, A., Gruber, N., Ishida, A., Joos, F., Key, R. M., Lindsay, K., Maier-Reimer, E., Matear,

- R. , Monfray, P., Mouchet, A., Najjar, R. G., Plattner, G-K, Rodgers, K. B., Sabine, C. L., Sarmiento, J. L. , Schlitzer, R., Slater, R. D., Totterdell, I. J., Weirig, M-F. , Yamanaka Y., Yoo, A, (2005). Anthropogenic ocean acidification over the twenty-first century and its impact on calcifying organisms, *Nature*, 437(7059), 681–686.
- Okin, G. S., Baker, A. R., Tegen, I. , Mahowald, N. M., Dentener, F. J., Duce, R. A., Galloway, J. N., Hunter, K., Kanakidou, M. , Kubilay, N., Prospero, J. M., Sarin, M., Surapipith, V., Uematsu, M., Zhu, T., (2011). Impacts of atmospheric nutrient deposition on marine productivity: Roles of nitrogen, phosphorus, and iron, *Global Biogeochemical Cycles*, 25:GB2022.
- Prentice, I. C., Farquhar, G. D., Fasham, M. J., Goulden, R. M., Heimann, L. M., Jaramillo, V. J., Khashgi, H. S., Le Quéré, C., Scholes, R. J. , Wallace, D.W.R., (2001). The carbon cycle and atmospheric carbon dioxide, in *Climate Change 2001: The Scientific Basis. Contribution of Working Group I to the Third Assessment Report of the Intergovernmental Panel on Climate Change*, edited by J. T. Houghton, Y. Ding, D. J. Griggs, M. Noguer, P. J. van der Linden, X. Dai, K. Maskell, and C.A. Johnson, pp. 183–237, Cambridge University Press, Cambridge, United Kingdom and New York, NY, USA.
- Platter, G.K., Knutti, R., Joos, F., Stocker, T.F., von Bloh, W., Brovkin, V., Cameron, D., Driesschaert, E., Dutkiewicz, S., Eby, M., Edwards, N.R., Fichefet, T., Hargreaves, J.C., Jones, C.D., Loutre, M.F., Matthews, H.D., Mouchet, A., Müller, S.A., Nawrath, S., Price, A., Sokolov, A., Strassmann, K.M., Weaver, A.J., (2008). Long-term climate commitments projected with climate-carbon cycle models, *Journal of Climate*, 21(12):2721-2751.
- Roe, G., (2009). Feedbacks, Timescales, and Seeing Red”, *The Annual Review of Earth and Planetary Sciences*, 37:93-115.
- Roeckner, E., Arpe, K., Bengtsson, L., Brinkop, S., Dumenil L, Esch M, Kirk E, Lunkeit F, Ponater M, Rockel B, Sausen R, Schlese U, Schubert S, Windelband M (1992). Simulation of the present-day climate with the ECHAM model: Impact of the model physics and resolution. *Max-Planck-Institut für Meteorologie, Hamburg*, 93:171.
- Sarmiento, J.L., and Le Quéré, C., (1996). Oceanic carbon dioxide uptake in a model of century-scale global warming, *Science*, 274:1346-1350.
- Sarmiento, J. L., Hughes, M. C., Stouffer, R. J., Manabe, S., (1998). Simulated response of the ocean carbon cycle to anthropogenic climate warming, *Nature*, 393: 245-249.
- Scheffer, M., Brovkin, V., Cox, P.M., (2006). Positive feedback between global warming and atmospheric CO₂ concentration inferred from past climate change, *Geophysical Research Letters*, 33:L10702.

- Schurgers, G., Mikolajewicz, U., Gröger, M., Maier-Reimer, E., Vizcaíno, M., Winguth, A., (2006). Dynamics of the terrestrial biosphere, climate and atmospheric CO₂ concentration during interglacials: a comparison between Eemian and Holocene, *Climate of the Past*, 2:205-220.
- Schurgers, G., Mikolajewicz, U., Gröger, M., Maier-Reimer, E., Vizcaíno, M., Winguth, A., (2007). The effect of land surface changes on Eemian climate, *Climate Dynamics*, 29:357–373.
- Schurgers, G., Mikolajewicz, U., Gröger, M., Maier-Reimer, E., Vizcaíno, M., Winguth, A., (2008). Long-term effects of biogeophysical and biogeochemical interactions between terrestrial biosphere and climate under anthropogenic climate change, *Global and Planetary Change*, 64:26–37.
- Scripps Institution of Oceanography, (2013). Concentrations of CO₂ in the Earth's atmosphere (parts per million) derived from in situ air measurements at the Mauna Loa Observatory, Hawaii: Latitude 19.5°N Longitude 155.6°W Elevation 3397m. Retrieved from <http://co2now.org/>, 15-03-2013.
- Sitch, S., Smith, B., Prentice, I.C., Arneth, A., Bondeau, A., Cramer, W., Kaplan, J.O., Levis, S., Lucht, W., Sykes, M.T., Thonicke, K., Venevsky, S., (2003). Evaluation of ecosystem dynamics, plant geography and terrestrial carbon cycling in the LPJ dynamic global vegetation model, *Global Change Biology*, 9:161-185.
- Sitch, S., Huntingford, C., Gedney, N., Levy, P.E., Lomas, M., Piao, S.L., Betts, R., Ciais, P., Cox, P., Friedlingstein, P., Jones, C.D., Prentice, I.C., Woodward, F.I., (2008). Evaluation of the terrestrial carbon cycle, future plant geography and climate-carbon cycle feedbacks using five Dynamic Global Vegetation Models (DGVMs), *Global Change Biology*, 14: 2015-2039.
- Tyndall, J., (1861). On the absorption and radiation of heat by gases and vapours, and on the physical connection, *Philosophical Magazine*, 22:277-302.
- Vizcaíno, M., Mikolajewicz, U., Gröger, M., Maier-Reimer, E., Schurgers, G., Winguth, A., (2008). Long-term ice sheet–climate interactions under anthropogenic greenhouse forcing simulated with a complex Earth System Model, *Climate Dynamics*, 31:665-690.
- Winguth, A., Mikolajewicz, U., Gröger, M., Maier-Reimer, E., Schurgers, G., Vizcaíno, M., (2005). Centennial-scale interactions between the carbon cycle and anthropogenic climate change using a dynamic Earth system model, *Geophysical Research Letters*, 32: L23714.

Institutionen för naturgeografi och ekosystemvetenskap, Lunds Universitet.

Student examensarbete (Seminarieuppsatser). Uppsatserna finns tillgängliga på institutionens geobibliotek, Sölvegatan 12, 223 62 LUND. Serien startade 1985. Hela listan och själva uppsatserna är även tillgängliga på LUP student papers (www.nateko.lu.se/masterthesis) och via Geobiblioteket (www.geobib.lu.se)

The student thesis reports are available at the Geo-Library, Department of Physical Geography and Ecosystem Science, University of Lund, Sölvegatan 12, S-223 62 Lund, Sweden. Report series started 1985. The complete list and electronic versions are also electronic available at the LUP student papers (www.nateko.lu.se/masterthesis) and through the Geo-library (www.geobib.lu.se)

- 230 Cléber Domingos Arruda (2011) Developing a Pedestrian Route Network Service (PRNS)
- 231 Nitin Chaudhary (2011) Evaluation of RCA & RCA GUESS and estimation of vegetation-climate feedbacks over India for present climate
- 232 Bjarne Munk Lyshede (2012) Diurnal variations in methane flux in a low-arctic fen in Southwest Greenland
- 233 Zhendong Wu (2012) Dissolved methane dynamics in a subarctic peatland
- 234 Lars Johansson (2012) Modelling near ground wind speed in urban environments using high-resolution digital surface models and statistical methods
- 235 Sanna Dufbäck (2012) Lokal dagvattenhantering med grönytefaktorn
- 236 Arash Amiri (2012) Automatic Geospatial Web Service Composition for Developing a Routing System
- 237 Emma Li Johansson (2012) The Melting Himalayas: Examples of Water Harvesting Techniques
- 238 Adelina Osmani (2012) Forests as carbon sinks - A comparison between the boreal forest and the tropical forest
- 239 Uta Klönne (2012) Drought in the Sahel – global and local driving forces and their impact on vegetation in the 20th and 21st century
- 240 Max van Meeningen (2012) Metanutsläpp från det smältande Arktis
- 241 Joakim Lindberg (2012) Analys av tillväxt för enskilda träd efter gallring i ett blandbestånd av gran och tall, Sverige
- 242 Caroline Jonsson (2012) The relationship between climate change and grazing by herbivores; their impact on the carbon cycle in Arctic environments
- 243 Carolina Emanuelsson and Elna Rasmusson (2012) The effects of soil erosion on nutrient content in smallholding tea lands in Matara district, Sri Lanka
- 244 John Bengtsson and Eric Torkelsson (2012) The Potential Impact of Changing Vegetation on Thawing Permafrost: Effects of manipulated vegetation on summer ground temperatures and soil moisture in Abisko, Sweden
- 245 Linnea Jonsson (2012). Impacts of climate change on Pedunculate oak and Phytophthora activity in north and central Europe
- 246 Ulrika Belsing (2012) Arktis och Antarktis föränderliga havsistäcken
- 247 Anna Lindstein (2012) Riskområden för erosion och näringsläckage i Segeåns

- avrinningsområde
- 248 Bodil Englund (2012) Klimatanpassningsarbete kring stigande havsnivåer i Kalmar läns kustkommuner
- 249 Alexandra Dicander (2012) GIS-baserad översvämningskartering i Segeåns avrinningsområde
- 250 Johannes Jonsson (2012) Defining phenology events with digital repeat photography
- 251 Joel Lilljebjörn (2012) Flygbildsbaserad skyddszonsinventering vid Segeå
- 252 Camilla Persson (2012) Beräkning av glaciärers massbalans – En metodanalys med fjärranalys och jämviktslinjehöjd över Storglaciären
- 253 Rebecka Nilsson (2012) Torkan i Australien 2002-2010 Analys av möjliga orsaker och effekter
- 254 Ning Zhang (2012) Automated plane detection and extraction from airborne laser scanning data of dense urban areas
- 255 Bawar Tahir (2012) Comparison of the water balance of two forest stands using the BROOK90 model
- 256 Shubhangi Lamba (2012) Estimating contemporary methane emissions from tropical wetlands using multiple modelling approaches
- 257 Mohammed S. Alwesabi (2012) MODIS NDVI satellite data for assessing drought in Somalia during the period 2000-2011
- 258 Christine Walsh (2012) Aerosol light absorption measurement techniques: A comparison of methods from field data and laboratory experimentation
- 259 Jole Forsmoo (2012) Desertification in China, causes and preventive actions in modern time
- 260 Min Wang (2012) Seasonal and inter-annual variability of soil respiration at Skyttorp, a Swedish boreal forest
- 261 Erica Perming (2012) Nitrogen Footprint vs. Life Cycle Impact Assessment methods – A comparison of the methods in a case study.
- 262 Sarah Loudin (2012) The response of European forests to the change in summer temperatures: a comparison between normal and warm years, from 1996 to 2006
- 263 Peng Wang (2012) Web-based public participation GIS application – a case study on flood emergency management
- 264 Minyi Pan (2012) Uncertainty and Sensitivity Analysis in Soil Strata Model Generation for Ground Settlement Risk Evaluation
- 265 Mohamed Ahmed (2012) Significance of soil moisture on vegetation greenness in the African Sahel from 1982 to 2008
- 266 Iurii Shendryk (2013) Integration of LiDAR data and satellite imagery for biomass estimation in conifer-dominated forest
- 267 Kristian Morin (2013) Mapping moth induced birch forest damage in northern Sweden, with MODIS satellite data
- 268 Ylva Persson (2013) Refining fuel loads in LPJ-GUESS-SPITFIRE for wet-dry areas - with an emphasis on Kruger National Park in South Africa
- 269 Md. Ahsan Mozaffar (2013) Biogenic volatile organic compound emissions from Willow trees
- 270 Lingrui Qi (2013) Urban land expansion model based on SLEUTH, a case

- study in Dongguan City, China
- 271 Hasan Mohammed Hameed (2013) Water harvesting in Erbil Governorate, Kurdistan region, Iraq - Detection of suitable sites by using Geographic Information System and Remote Sensing
- 272 Fredrik Alström (2013) Effekter av en havsnivåhöjning kring Falsterbohalvön.
- 273 Lovisa Dahlquist (2013) Miljöeffekter av jordbruksinvesteringar i Etiopien
- 274 Sebastian Andersson Hylander (2013) Ekosystemtjänster i svenska agroforestrysystem
- 275 Vlad Pirvulescu (2013) Application of the eddy-covariance method under the canopy at a boreal forest site in central Sweden
- 276 Malin Broberg (2013) Emissions of biogenic volatile organic compounds in a Salix biofuel plantation – field study in Grästorps (Sweden)
- 277 Linn Renström (2013) Flygbildsbaserad förändringsstudie inom skyddszoner längs vattendrag
- 278 Josefin Methi Sundell (2013) Skötsel effekter av miljöersättningen för natur- och kulturmiljöer i odlingslandskapets småbiotoper
- 279 Kristín Agustsdóttir (2013) Fishing from Space: Mackerel fishing in Icelandic waters and correlation with satellite variables
- 280 Cristián Escobar Avaria (2013) Simulating current regional pattern and composition of Chilean native forests using a dynamic ecosystem model
- 281 Martin Nilsson (2013) Comparison of MODIS-Algorithms for Estimating Gross Primary Production from Satellite Data in semi-arid Africa
- 282 Victor Strevens Bolmgren (2013) The Road to Happiness – A Spatial Study of Accessibility and Well-Being in Hambantota, Sri Lanka
- 283 Amelie Lindgren (2013) Spatiotemporal variations of net methane emissions and its causes across an ombrotrophic peatland - A site study from Southern Sweden
- 284 Elisabeth Vogel (2013) The temporal and spatial variability of soil respiration in boreal forests - A case study of Norunda forest, Central Sweden
- 285 Cansu Karsili (2013) Calculation of past and present water availability in the Mediterranean region and future estimates according to the Thornthwaite water-balance model
- 286 Elise Palm (2013) Finding a method for simplified biomass measurements on Sahelian grasslands
- 287 Manon Marcon (2013) Analysis of biodiversity spatial patterns across multiple taxa, in Sweden
- 288 Emma Li Johansson (2013) A multi-scale analysis of biofuel-related land acquisitions in Tanzania - with focus on Sweden as an investor